On the Tuning of Predictive Controllers: Impact of Disturbances, Constraints, and Feedback Structure

Benjamin P. Omell and Donald J. Chmielewski
Dept. of Chemical and Biological Engineering, Illinois Institute of Technology, Chicago, IL 60616

DOI 10.1002/aic.14529
Published online July 3, 2014 in Wiley Online Library (wileyonlinelibrary.com)

The impact of problem formulation modifications on predictive controller tuning is investigated. First, the proposed tuning method is shown to adapt to disturbance characteristic changes and thus, takes full economic advantage of the scenario. The second topic concerns point-wise-in-time constraints and the impact of constraint infeasibility. Specifically, we shift the tuning question from selection of nonintuitive weighting matrix parameters to that of a few key parameters and results in a rather intuitive trade-off between expected profit and expected constraint violations. Finally, we show that simple modifications will allow for the consideration of various feedback structures, including computational delay and partial state information. The overall conclusions of the work are that the results of the automated algorithm will help build an intuitive understating of the dynamics of the process and ultimately result in a higher level trade-off between profit and constraint observance. © 2014 American Institute of Chemical Engineers *AIChE J*, 60: 3473–3489, 2014

Keywords: linear matrix inequalities, model predictive control, optimization, process control, process economics

Introduction

The economic impact of a control system has long been of interest to the process systems engineering community. From the perspective of process design and optimization, the goal is to design equipment and select operating conditions that will minimize a combination of capital and operating costs. To address uncertainty issues, methods have been developed to mimic the actions of a control system. The most popular approach is that of flexibility analysis, which can be further divided into deterministic methods[1–9] and stochastic methods.[10–14] Another method that is growing in popularity is that of chance constrained optimization.[15–21] If one assumes a given set of equipment and equipment size specifications, then the questions focuses on the economic impacts of control structure and operating point selection. The subject of control structure selection can be further divided into plant-wide control[22–27] and the selection of measurements and manipulations.[28–41] Operating point selection methods can also be divided into subcategories. Methods employing a constant-in-time uncertainty perspective[42–48] are akin to deterministic flexibility analysis. Those with a time-dependent uncertainty perspective[49–55] are related to the stochastic flexibility and chance constrained approaches. It is interesting to note that some of the above methods fall into both categories, in the sense that control structure is the objective, but operating point selection is motivated by process economics.[32,34,36,41]

Correspondence concerning this article should be addressed to D. J. Chmielewski at chmielewski@iit.edu.

The scope of the current effort assumes all equipment has been specified (including measurement and manipulation equipment) and a two-stage control system structure will be used. More specifically, a multi-input multioutput model predictive controller (MPC) is assumed to receive set-point commands from a real-time optimizer (RTO). However, in contrast to many industrial implementations (but aligned with the operating point selection literature cited earlier), the RTO will be equipped with a back-off operating point (BOP) selection procedure. The interaction of the three decision units is illustrated in Figure 1. Using the constant-in-time uncertainties (determined by a parameter estimator), a steady-state version of the process model and a set of operating constraints, the RTO will determine an optimal steady-state operating point (OSSOP). Then, the BOP selection procedure will consider the time-dependent aspects of the uncertainties to determine the regulatory performance expected from the MPC. This regulatory performance can be visualized (see Figure 2) as an elliptical operating region around the selected BOP and is denoted as the expected dynamic operating region (EDOR). Then, the procedure selects a BOP such that the economics of the process are optimized while ensuring that all points of the EDOR satisfy the operating constraints. This BOP is then sent to the MPC, which it uses as the operating target. The motivation for a BOP selection procedure is to provide the MPC with a set-point that is close to the OSSOP, but a sufficient distance from the inequality constraints.

A distinctive feature of the BOP selection procedure of Ref. 51 is that the regulatory performance of the controller is variable. This ability to change the tuning parameters of the controller provides greater freedom in the selection of a BOP and thus will result in lower operating costs (see

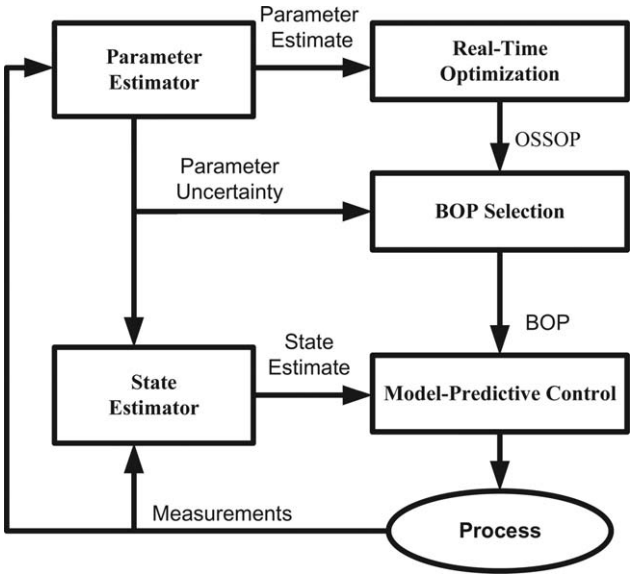

Figure 1. Three-stage control structure.

Figure 3). The purpose of this article is to explore the effects of numerous design issues that arise in MPC design and in particular, the adaptive nature of the MPC tuning methods presented in Ref. 51. As a point of comparison, the results of the proposed method will be contrasted with those of the fixed controller BOP selection procedures.[37]

In the remainder of this section, the method of Ref. 51 will be reviewed and the illustrative example of a two-Continuously Stirred Tank Reactor (two-CSTR) process will be introduced. In the Statistically Constrained Control Section, the simple extensions of disturbance modeling and the discrete-time formulation will be discussed. Using the two-CSTR example, we will also illustrate how method of Ref. 51 is able to adapt the controller to the expected disturbance characteristics. In the Predictive Control with Full State Information Section, the method of inverse optimality will be used to construct a predictive controller with an EDOR similar to that specified by the free controller BOP selection problem of Ref. 51. This section will also illustrate the use of a soft constrained MPC formulation (to address infeasible initial conditions) and discuss how a redefinition of the EDOR will create a trade-off between expected profit and the occurrence of infeasibilities. The section will conclude with a short illustration of the impact of mismatch in the disturbance model. The Modifications to the Measurement Structure Section will illustrate how to modify the controller formulation to accommodate changes in the measurement structure. The article concludes with a short discussion on the impact of process nonlinearities and an *ad hoc* approach to correct for these discrepancies.

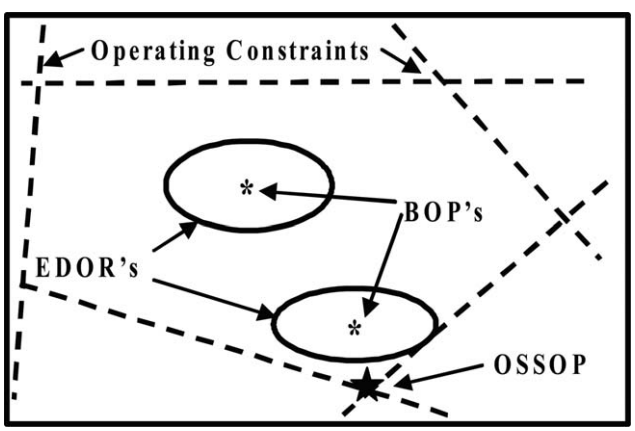

Figure 2. Visualization of the EDOR.

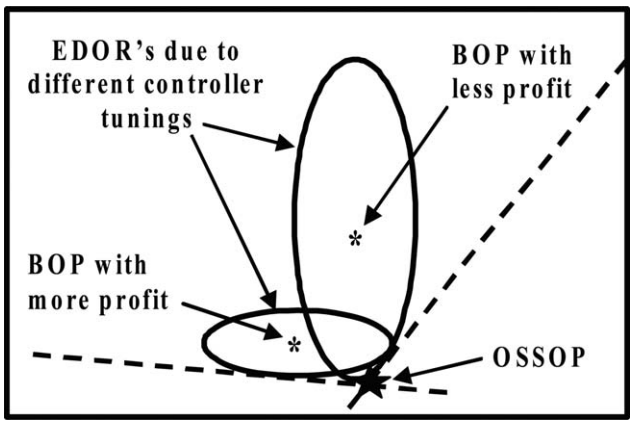

Figure 3. Simultaneous BOP selection and controller design.

Review of simultaneous BOP selection and controller design

Consider a nonlinear process model: $\dot{s}=f(s,m,p)$, $q=h(s,m,p)$, and $q^{\min} \le q \le q^{\max}$ where s, m, p, and q are the state, manipulated, disturbance, and performance variables (each a column vector of dimension n_s, n_m, n_p, and n_q, respectively). The RTO will use a steady-state version of this model to determine the OSSOP, based on an operating cost function $g(q)$, operating constraints $q^{\min} \le q \le q^{\max}$ and an assumed constant-in-time value for the disturbance, $p = p^{\text{ossop}}$. Clearly, if an element of s or m appears explicitly in the economics of the process or is constrained, then these variables can be included in the set of performance variables q

$$\begin{aligned} &\min_{s,m} \{g(q)\} \quad \text{s.t.} \\ &0=f(s,m,p^{\text{ossop}}) \\ &q=h(s,m,p^{\text{ossop}}) \\ &q^{\min} \le q \le q^{\max} \end{aligned} \tag{1}$$

The solution to this nonlinear optimization is the OSSOP and is denoted by the triple (s^{OSSOP}, m^{OSSOP}, q^{OSSOP}). The next step is to determine the appropriate amount of back-off. The BOP will be denoted as (s^{BOP}, m^{BOP}, q^{BOP}), which leads to the following deviation variables with respect to the OSSOP: $s'=s^{\text{BOP}}-s^{\text{OSSOP}}$, $m'=m^{\text{BOP}}-m^{\text{OSSOP}}$, $q'=q^{\text{BOP}}-q^{\text{OSSOP}}$ and $p'=p^{\text{BOP}}-p^{\text{OSSOP}}$. Using these definitions, the profit function can be approximated with the following linearization

$$g\left(q^{\text{BOP}}\right) \cong g\left(q^{\text{OSSOP}}\right)+g_q^T q' \tag{2}$$

where g_q is the partial derivative of $g(q)$ evaluated at the OSSOP and the term $g_q^T q'$ approximates profit lost. The set of available BOPs, which must be steady-state operating points, can be approximated by

$$0=As'+Bm' \tag{3}$$

$$q'=D_x s'+D_u m' \tag{4}$$

where A, B, G, D_x, D_u, are the system matrices of the process linearized around the OSSOP and $p'=0$ if we assume $p^{\mathrm{BOP}}=p^{\mathrm{OSSOP}}$, which need not be the case (see Ref. 56 for an example). The distance between the BOP and the constraints is given by $q^{\mathrm{BOP}}-q^{\min}$ on one side and $q^{\max}-q^{\mathrm{BOP}}$ on the other. However, if one defines $q'^{\min}=q^{\min}-q^{\mathrm{OSSOP}}$ and $q'^{\max}=q^{\max}-q^{\mathrm{OSSOP}}$, then the distance between the BOP and the constraints is also given by $q'-q'^{\min}$ and $q'^{\max}-q'$. As a feasible BOP will have both of these quantities positive, the inequality constraints in deviation variables with respect to the OSSOP are

$$q'^{\min} \le q' \le q'^{\max} \tag{5}$$

Turning to the dynamic perspective, the BOP will serve as the target point for the controller and all of its actions will be to drive the system toward the BOP. Thus, the variables seen by the controller should be deviation variables with respect to the BOP, defined as $x=s-s^{\mathrm{BOP}}$, $u=m-m^{\mathrm{BOP}}$, $w=p-p^{\mathrm{BOP}}$, and $z=q-q^{\mathrm{BOP}}$, which results in the following linearized dynamic model

$$\dot{x}=Ax+Bu+Gw \tag{6}$$

$$z=D_x x+D_u u+D_w w \tag{7}$$

Note that the system matrices of (6) and (7) are the same as those used in (3) and (4). This suggests the system is linearized around the OSSOP and not the BOP, which will result in a less accurate EDOR predicted by the linear model. This can easily be remedied by linearizing around the BOP, however, difficulty arises because the BOP is only known after the EDOR is determined. For the moment, we will accept this discrepancy and return to this issue in The Impact of Nonlinearities Section. Now, assume the controller is known to be $u=Lx$, where L is given. Furthermore, assume w is a zero-mean white noise process with a spectral density S_w. Then, the EDOR is defined by the following relations

$$\Sigma_x(A+BL)^T+(A+BL)\Sigma_x+GS_wG^T=0 \tag{8}$$

$$\Sigma_z=(D_x+D_uL)\Sigma_x(D_x+D_uL)^T+D_wS_wD_w{}^T \tag{9}$$

$$\zeta_j=\rho_j\Sigma_z\rho_j^T, \quad j=1\ldots n_q \tag{10}$$

$$\sigma_j=\sqrt{\zeta_j}, \quad j=1\ldots n_q \tag{11}$$

where ρ_j is the jth row of an $n_q \times n_q$ identity matrix. The size of the EDOR in the jth direction is defined as $\alpha\sigma_j$, where α is a scaling factor indicating how many standard deviations will be used to define the EDOR ($\alpha=1$ unless specified otherwise). Next, we will need to exclude any BOP such that the associated EDOR is not contained in the region defined by $q^{\min}$ and $q^{\max}$. As such a BOP is feasible if

$$\alpha\sigma_j \le q_j'-q_j'^{\min} \quad \text{and} \quad \alpha\sigma_j \le q_j'^{\max}-q_j' \tag{12}$$

Finally, the BOP is found as the solution to the following linear program

$$\begin{aligned} &\min_{s',m',q'} \left\{ g_q^T q' \right\} \quad \text{s.t.} \\ &(3),(4),(5), \text{ and } (12) \end{aligned} \tag{13}$$

It is important to note that as far as the linear program is concerned, the σ_is are constants that are calculated only once using Eqs. 8–11. This fixed controller approach to BOP selection is closely related to the procedure of Loeblein and Perkins.[37]

It is noted that the linearization steps of Eqs. 2–4 are not required, but serve to reduce the computational complexity of problem (13). Specifically, the original nonlinear objective and nonlinear process model, both with respect to the steady-state process variables, may be retained. In this case, problem (13) will be, in general, a nonlinear program and require a solution method similar to that used for problem (1). Further investigation of this class of problems will be the subject of future work. It is further highlighted that the linearization step of Eqs. 6 and 7 is required for the procedure. Without such a linearization a Fokker–Planck type formulation will be required to calculate the variances used to define the EDOR. Although this may be computationally tractable for the above fixed controller case, a nonlinear approach will be intractable in the free controller case described next.

The free controller BOP selection problem is simply an augmentation of problem (13) with Eqs. 8–11. The result is the ability to change the shape of the EDOR (through modification of the controller) while simultaneously moving the BOP. The modifications result in the following nonlinear program[51]

$$\begin{aligned} &\min_{s',m',q',\zeta_j,\sigma_j,\Sigma_x,L} \left\{ g_q^T q' \right\} \quad \text{s.t.} \\ &(3),(4),(5),(8),(9),(10),(11), \text{ and } (12) \end{aligned} \tag{14}$$

Through application of Theorem 3.1 of Ref. 57, the nonlinear equality constraints of (8)–(10) can be replaced by convex linear matrix inequality constraints with no change to the BOP feasible region. The resulting free controller BOP selection problem is as follows

$$\min_{s',m',q',\sigma_j,\zeta_j,X>0,Y} \left\{ g_q^T q' \right\} \quad \text{s.t.} \tag{15}$$

$$0=As'+Bm', \;\; q'=D_xs'+D_um', \;\; q'^{\min} \le q' \le q'^{\max} \tag{16}$$

$$\alpha\sigma_j \le q_j'^{\max}-q_j', \;\; \alpha\sigma_j \le q_j'-q_j'^{\min}, \;\; j=1\ldots n_q \tag{17}$$

$$\zeta_j=\sigma_j{}^2, \quad j=1\ldots n_q \tag{18}$$

$$(AX+BY)+(AX+BY)^T+GS_wG^T<0 \tag{19}$$

$$\begin{bmatrix} \zeta_j & \rho_j(D_xX+D_uY) \\ (D_xX+D_uY)^T\rho_j{}^T & X \end{bmatrix} > 0, \quad j=1\ldots n_q \tag{20}$$

To address the reverse-convex constraints of (18), Ref. 51 proposes a global solution procedure based on the branch and bound algorithm.

Two-CSTR case study

The reactor process of Figure 4, adapted from Ref. 36, will be used to illustrate the features of the free controller BOP selection method. The process consists of two, jacket-cooled CSTRs in series with an intermediate feed. In both reactors, two irreversible, exothermic, first-order reactions take place, $A \rightarrow B \rightarrow C$, where species C is undesired. The goal of the process is to maximize profit by manipulating volumetric flow rates in the face of uncertainties associated with feed temperature, feed concentration, cooling water temperatures, and reaction kinetics. The process is described by the following material and energy balances

$$\frac{dC_{A,1}}{dt}=\frac{Q_1\left(C_{A,F}-C_{A,1}\right)}{V}-r_A\left(T_1,C_{A,1}\right) \tag{21}$$

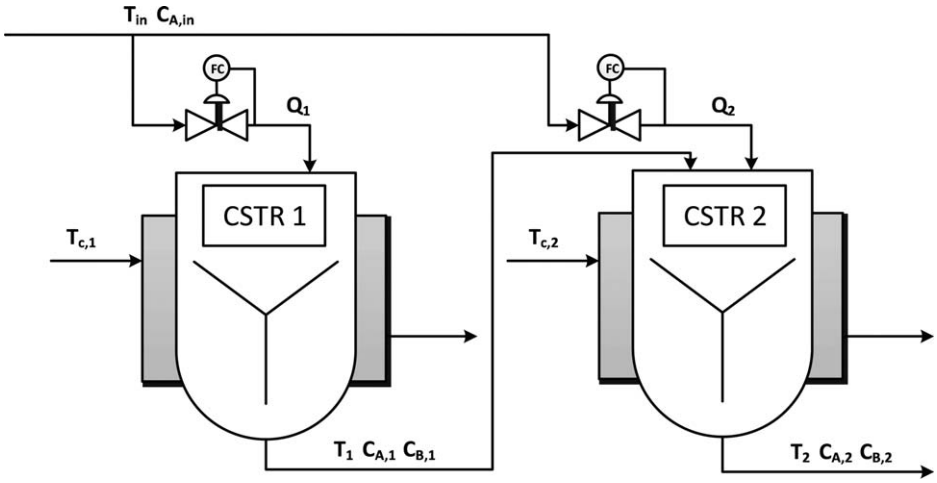

Figure 4. Process diagram for the two-CSTR process.

$$\frac{dC_{B,1}}{dt} = -\frac{Q_1 C_{B,1}}{V} + r_A\left(T_1, C_{A,1}\right) - r_B\left(T_1, C_{B,1}\right) \tag{22}$$

$$\frac{dT_1}{dt} = \frac{Q_1(T_F - T_1)}{V} - H_A r_A\left(T_1, C_{A,1}\right) - H_B r_B\left(T_1, C_{B,1}\right) - q_{c,1}/V \tag{23}$$

$$\frac{dC_{A,2}}{dt} = \frac{Q_1 C_{A,1} + Q_2 C_{A,F} - Q_T C_{A,2}}{V} - r_A\left(T_2, C_{A,2}\right) \tag{24}$$

$$\frac{dC_{B,2}}{dt} = \frac{Q_1 C_{B,1} - Q_T C_{B,2}}{V} + r_A\left(T_2, C_{A,2}\right) - r_B\left(T_2, C_{B,2}\right) \tag{25}$$

$$\frac{dT_2}{dt} = \frac{Q_1 T_1 + Q_2 T_F - Q_T T_2}{V} - H_A r_A\left(T_2, C_{A,2}\right) - H_B r_B\left(T_2, C_{B,2}\right) - q_{c,2}/V \tag{26}$$

where $r_A(T, C_A) = C_A k_I \exp\left(-\frac{E_{A,I}}{RT}\right)$, $r_B(T, C_B) = C_B k_{II} \exp\left(-\frac{E_{A,II}}{RT}\right)$, $q_{c,j} = U_a\left(T_j - T_{c,j}\right)$, and $Q_T = Q_1 + Q_2$. (See Table 1 for parameter values.)

Instantaneous profit is calculated as the rate of product B leaving the system minus the cost of feed material and utilities (reactor cooling)

$$g = 10 C_{B,2} Q_T - 0.1 Q_T - 0.01 q_{c,1} - q_{c,2} \tag{27}$$

The difference in utility cost coefficients for $q_{c,1}$ and $q_{c,2}$ stems from the fact that the cooling fluid in tank two is chilled below ambient temperature (nominally $T_{c,1} = 310$ K and $T_{c,2} = 288$ K). The operating constraints are as follows: $T_1 \le 350$ K, $T_2 \le 350$ K, $q_{c,1} \le 30$ m^{3}K/s, $q_{c,2} \le 17.5$ m^{3}K/s, $Q_T \le 0.8$ m^3/s, $Q_1 \ge 0.1$ m^3/s, $Q_2 \ge 0.1$ m^3/s, and $0 \le C_{A,2} \le 0.3$ kmol/m^3. The above model can be put into the form of problem (1) by the following definitions

$$s = [C_{A,1} \quad C_{B,1} \quad T_1 \quad C_{A,2} \quad C_{B,2} \quad T_2]^T$$

$$m = [Q_1 \quad Q_2]^T$$

$$p = [T_F \quad C_{A,F} \quad T_{c,1} \quad T_{c,2} \quad k_{II}]^T$$

$$q = [T_1 \quad C_{A,2} \quad C_{B,2} \quad T_2 \quad Q_T \quad Q_1 \quad Q_2 \quad q_{c,1} \quad q_{c,2}]^T$$

Statistically Constrained Control

In this section, the specifics of BOP selection and controller design using the methods of Ref. 51 are illustrated. In particular, the method is compared to the fixed controller case, the impact of disturbance modeling is illustrated and the discrete-time framework is discussed.

Fixed vs. free controller back-off

The first step in calculating the optimal back-off for both the fixed and free controller methods is to find the OSSOP by solving problem (1). For this study, it is assumed that the parameter estimator has identified the following nominal values for the disturbance vector $p^{\text{OSSOP}} = [300 \ 20 \ 310 \ 288 \ 160]^T$, where the units of p are [K kmol/m^3 K K s^{-1}]. The resulting OSSOP is given by $m^{\text{OSSOP}} = [0.283 \ 0.232]^T$ m^3/s and gives a profit of \$83.65/h with active constraints at T_1 and $q_{c,2}$.

Linearization of (21)–(26) around the OSSOP will result in the following system matrices where the submatrices are given in Appendix

$$A = \begin{bmatrix} A_{11} & 0 \\ A_{21} & A_{22} \end{bmatrix}, \ B = \begin{bmatrix} B_1 \\ B_2 \end{bmatrix}, \ G = \begin{bmatrix} G_1 \\ G_2 \end{bmatrix} \tag{28}$$

$$D_x = \begin{bmatrix} D_{x,1} \\ 0 \\ D_{x,3} \end{bmatrix}, \ D_u = \begin{bmatrix} 0 \\ D_{u,2} \\ 0 \end{bmatrix}, \ D_w = \begin{bmatrix} 0 \\ 0 \\ D_{w,3} \end{bmatrix} \tag{29}$$

The disturbance, w, is assumed to be zero-mean white noise with spectral density, S_w, equal to diag{49 2 36 36 4}. Assume the controller used in the fixed controller case is $L = -R^{-1}B^T P$ where P is the positive definite solution to the Riccati equation $0 = A^T P + PA + Q - PBR^{-1}B^T P$, $Q = I$ and $R = I$. Then, the standard deviation of the performance outputs is calculated using (8)–(11) and finally problem (13) is

Table 1. Parameter Values

Parameter	Value
k_I	2.7×10^8 s^{-1}
k_{II}	160 s^{-1}
$E_{A,I}/R$	6000 K
$E_{A,II}/R$	4500 K
H_A	-5 m^3 K/kmol
H_B	-5 m^3 K/kmol
U_a	0.35 m^3/s
V	5 m^3

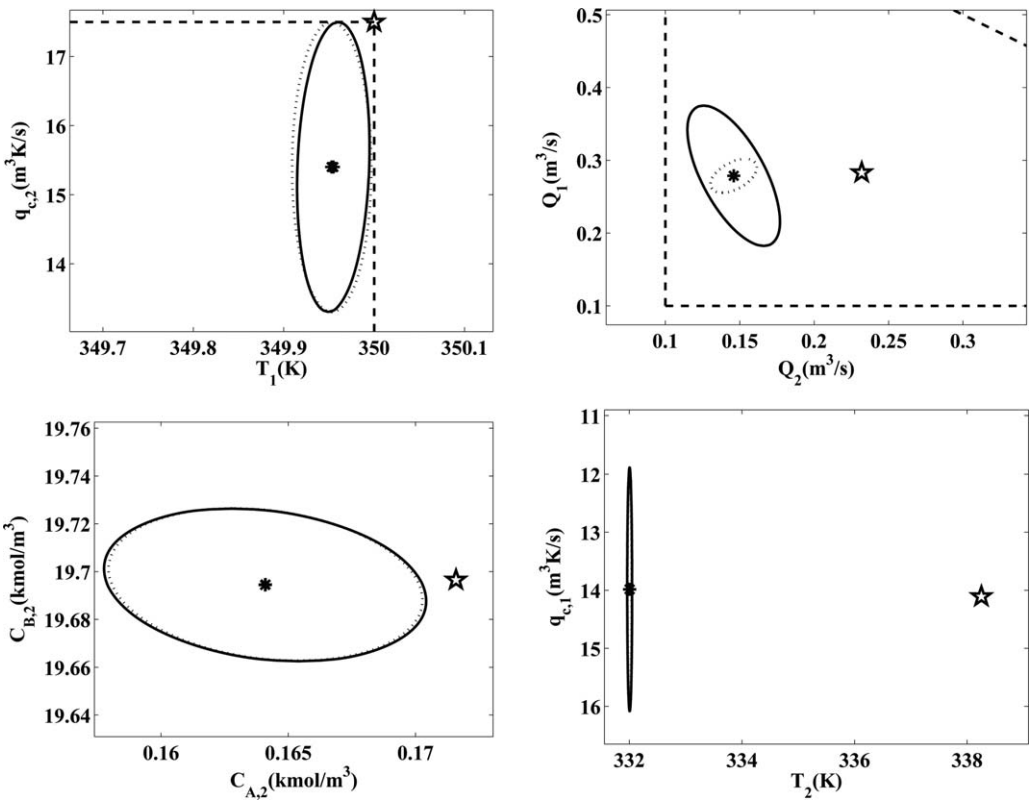

Figure 5. Comparison of BOPs and EDORs for the fixed controller (dotted) and free controller (solid).

solved. In the free controller case, problem (15) is solved. If the solution to (15) is X^*, Y^*, then a feasible linear feedback is $L = Y^*(X^*)^{-1}$.

A comparison of the two cases is given in Figure 5. The eight-dimensional ellipse, the EDOR, is simply the solution to $(q-q^{\mathrm{BOP}})\Sigma_z^{-1}(q-q^{\mathrm{BOP}})^T=\alpha^2$, where Σ_z is from (8) to (9) using the respective controller. The five-point star gives the OSSOP and the * point is the BOP. Notice that the EDOR is far from the constraints in the $C_{A,2}$, $C_{B,2}$, T_2, and $q_{c,1}$ directions (the bottom two plots). In the fixed controller case, rather tight regulation is achieved in both the T_1 and T_2 directions, whereas fairly loose regulation occurs in the $q_{c,1}$ and $q_{c,2}$ directions. This is to be expected as $q_{c,1}$ and $q_{c,2}$ are not state variables and thus are not explicitly included in the linear quadratic regulator (LQR) objective used to calculate the fixed controller. In the case of $q_{c,2}$ (the expensive utility), the required back-off (to approximately 15.5 m^{3}K/s) is achieved by reducing the steady-state value of T_2, which results from reducing Q_2 to about 0.15 m^3/s. The free controller optimization indicates that the fixed controller is doing about the best one could expect under the given situation, although this conclusion would be difficult to determine without the free controller analysis. The only difference between the two is that the free controller method selects a controller with slightly tighter regulation in the T_1 direction in an effort to get the BOP closer to the OSSOP in that direction. The result is a very slight reduction in profit loss with respect to the OSSOP, \$15.63/h for the fixed controller case and \$15.61/h for the free controller. Recalling that profit at the OSSOP is \$83.65/h, the profits are \$68.02/h and \$68.04/h for the fixed and free cases, respectively. Although these two controllers show similar performance, the next subsection will show that the fixed controller does not adapt as well to changes in the disturbance characteristics.

Impact of disturbance modeling

A technical issue associated with the example of the previous subsection concerns the selection of the spectral density S_w. The concern stems from the fact that white noise contains all frequencies and has infinite variance. However, the disturbances acting on a process are unlikely to have such characteristics. To alleviate this issue, first-order shaping filters are used for each of the disturbances acting on the two-CSTR process. These will be of the form $\tau_f\dot{x}_f=w-x_f$, where x_f is the filter output, w is white noise, and τ_f is the correlation time of the disturbance. Applying Eq. 8 to this process results in the following calculation of steady-state variance for x_f: $\Sigma_f = S_w/2\tau_f$. Thus, if one would like a disturbance x_f to have a variance Σ_f then the spectral density should be selected as $S_w = 2\tau_f\Sigma_f$. The impact of this relation is that one can use process measurements to identify the correlation time and variance of the disturbance and thus arrive at a meaningful value for S_w.

To incorporate into the two-CSTR model, define the following: $G_f = \mathrm{diag}\{1/\tau_{f1},\ldots,1/\tau_{f5}\}$ and $A_f = -G_f$. Then, the system matrices should be constructed as

$$A=\begin{bmatrix} A_{11} & 0 & G_1 \\ A_{21} & A_{22} & G_2 \\ 0 & 0 & A_f \end{bmatrix},\quad B=\begin{bmatrix} B_1 \\ B_2 \\ 0 \end{bmatrix},\quad G=\begin{bmatrix} 0 \\ 0 \\ G_f \end{bmatrix}$$

$$D_x=\begin{bmatrix} D_{x,1} & 0 \\ 0 & 0 \\ D_{x,3} & D_{w,3} \end{bmatrix},\quad D_u=\begin{bmatrix} 0 \\ D_{u,2} \\ 0 \end{bmatrix},\quad D_w=0$$

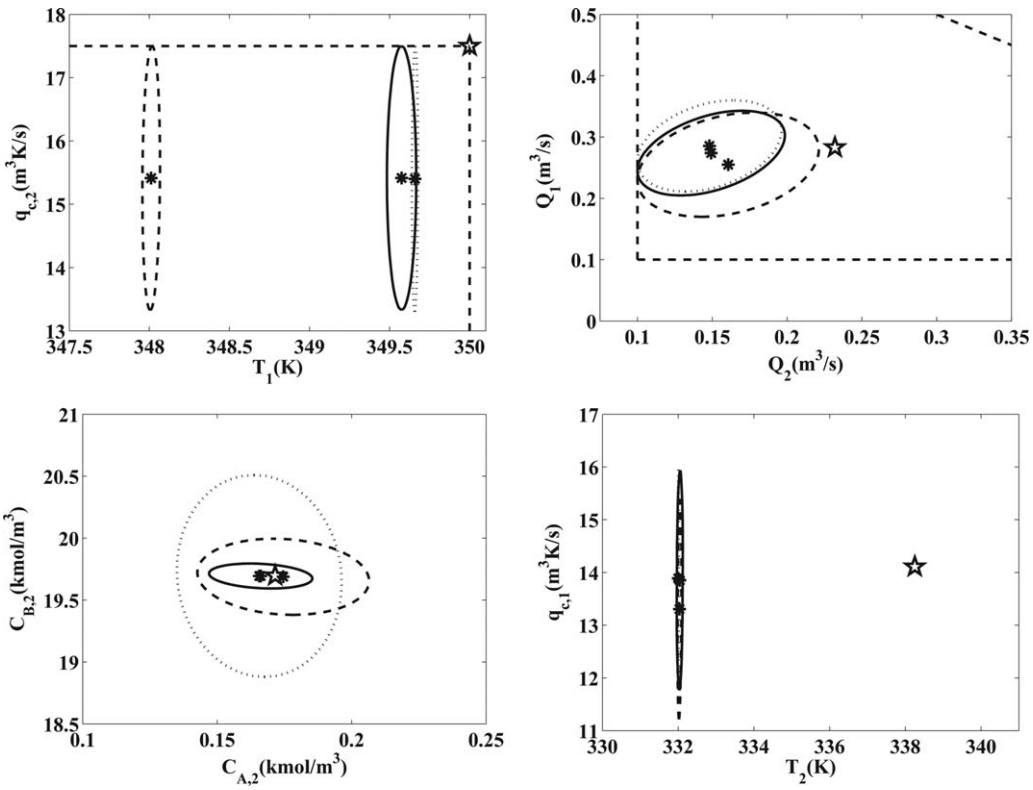

Figure 6. Impact of disturbance correlation time (τ_f) on fixed controller BOPs and EDORs (solid $\tau_f = 0.1$ s, dashed $\tau_f = 1$ s, and dotted $\tau_f = 10$ s).

It is important to note that in the example of the previous subsection, the above approach was used in place of true white noise disturbances. Specifically, S_w was set equal to $2\tau_f\Sigma_f$ where $\Sigma_f = \text{diag}[49\ 2\ 36\ 36\ 4]$ and $\tau_f = 0.01$ s ($\tau_{fi} = \tau_f$ $i = 1\ldots5$). Due to the very small correlation time, the resulting disturbances were good approximations of white noise, but had finite variances equal to those specified by Σ_f.

Figure 6 illustrates how changes to τ_f will impact the selected BOP in the fixed controller case. It is important to note that due to our definition of spectral density, $S_w = 2\tau_f\Sigma_f$, the variances of the disturbances acting on the process remain constant regardless of the τ_f value used. As τ_f increases, the disturbances will change more slowly with respect to time, which should allow the controller to achieve better performance. However, in the fixed controller case, performance degrades and then eventually improves as visualized by the movement of the BOP in the T_1 direction. Quantitatively, the fixed controller profit loss is \$15.94/h for $\tau_f = 0.1$, \$17.64/h for $\tau_f = 1$, and \$15.93/h for $\tau_f = 10$ (Table 2). Although this sort of behavior seems unnatural, there is a logic to the fixed controller solutions. First, recall that the EDOR for each value of τ_f is constant and that the fixed controller optimization can change only the BOP. Second, note that the $q_{c,2}$ direction dominates the economics of the process. Thus, given the $q_{c,2}$ standard deviation, the optimal BOP in the $q_{c,2}$ direction is about 15.5 m^3/s. This is made possible by reducing the BOP in the T_2 direction to about 332 K, which is achieved by reducing the Q_2 BOP. However, this reduction is limited by the Q_2 EDOR and the constraint $Q_2 \geq 0.1$ (see top right plot). Thus, the core issue is how much the Q_2 BOP can change when the Q_2 EDOR changes due to changes in τ_f. Clearly, the Q_2 EDOR is largest when $\tau_f = 1$. The impact is that the BOP in the Q_2 direction is a bit larger, which should cause the BOP in the T_2 direction to increase. It does not increase because the $q_{c,2}$ constraint would become violated, so it opts to decrease T_1, by decreasing the BOP in the Q_1 direction.

In the free controller case of Figure 7, this connection between Q_1 and $q_{c,2}$ is exploited, especially as τ_f increases. Consider the $\tau_f = 10$ case. If the instantaneous value of the disturbance $T_{c,2}$ decreases, then the controller will try to decrease T_2, to satisfy the $q_{c,2}$ constraint, by decreasing T_1 (through manipulation of Q_1) as well as through the more direct route of manipulating Q_2. These additional manipulations are observed by the substantially increased EDOR in the Q_1 and Q_2 directions. The end result is that the EDOR in the $q_{c,2}$ direction is reduced and thus allows the $q_{c,2}$ BOP to be closer to the OSSOP. The fact that the T_1 BOP must be further from the OSSOP is immaterial as the T_1 direction has much less influence on the economics of the process. It is also interesting to note that profit loss for the free controller case is monotonic with respect to τ_f: \$15.61/h for $\tau_f = 0.1$, \$14.28/h for $\tau_f = 1$, and \$7.29/h for $\tau_f = 10$.

Discrete-time formulation

To arrive at a discrete-time formulation, the first step is to convert the dynamic model to discrete-time form. One

Table 2. Profit Loss vs. Disturbance Characteristics

Disturbance Characteristics	Fixed Controller Profit Loss (\$/h)	Free Controller Profit Loss (\$/h)
White Noise	15.63	15.61
$\tau = 0.1$ s	15.94	15.61
$\tau = 1$ s	17.04	14.28
$\tau = 10$ s	15.93	7.42

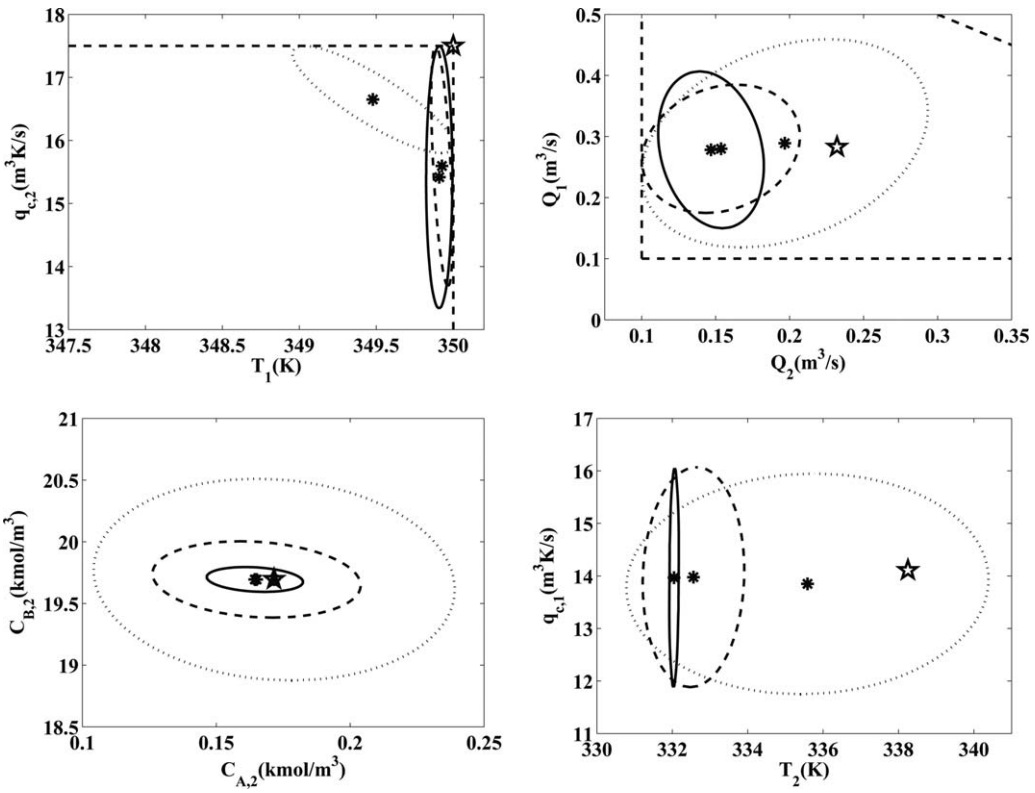

Figure 7. Impact of disturbance correlation time (τ_f) on free controller BOPs and EDORs (solid $\tau_f = 0.1$ s, dashed $\tau_f = 1$ s, and dotted $\tau_f = 10$ s).

approach is to use the method of sample and hold[58] to arrive at

$$x_{i+1} = A_d x_i + B_d u_i + G_d w_i \tag{30}$$

where $x_i = x(i\Delta t)$, $u(t) = u_i$, $i\Delta t \le t < (i+1)\Delta t$, $w(t)$ is similarly defined, w_i is a white noise sequence with variance Σ_w and Δt is the sample time. The system matrices are calculated as $A_d = e^{A\Delta t}, B_d = \left(\int_0^{\Delta t} e^{A\tau} d\tau\right) B, G_d = \left(\int_0^{\Delta t} e^{A\tau} d\tau\right) G$, and $\Sigma_w = S_w/\Delta t$. The second step is to replace the steady-state model constraint, $0 = As' + Bm' + Gp'$, with its discrete-time equivalent: $s' = A_d s' + B_d m' + G_d p'$. The third step is to convert the covariance analysis to discrete-time. Specifically, Eq. 8 is replaced with $\Sigma_x = (A_d + B_d L)\Sigma_x (A_d + B_d L)^T + G_d \Sigma_w G_d{}^T$. Then, application of Theorem 6.1 of Ref. 57 results in the following discrete-time version of the free controller BOP selection problem

$$\min_{s',m',q',\sigma_j,\zeta_j,X>0,Y} \left\{ g_q^T q' \right\} \quad \text{s.t.} \tag{31}$$

$$s' = A_d s' + B_d m', \;\; q' = D_x s' + D_u m', \;\; q'^{\min} \le q' \le q'^{\max} \tag{32}$$

$$\alpha\sigma_j \le q_j'^{\max} - q_j', \;\; \alpha\sigma_j \le q_j' - q_j'^{\min}, \quad j = 1 \ldots n_q \tag{33}$$

$$\zeta_j = \sigma_j{}^2, j = 1 \ldots n_q \tag{34}$$

$$\begin{bmatrix} X - G_d \Sigma_w G_d^T & A_d X + B_d Y \\ (A_d X + B_d Y)^T & X \end{bmatrix} > 0 \tag{35}$$

$$\begin{bmatrix} \zeta_j & \rho_j (D_x X + D_u Y) \\ (D_x X + D_u Y)^T \rho_j{}^T & X \end{bmatrix} > 0, \quad j = 1 \ldots n_q \tag{36}$$

Figure 8 illustrates that for small sample-times the BOP and EDOR resulting from the discrete-time formulation are nearly identical to those of the continuous-time formulation, although, for larger sample-times the impact is significant. For $\Delta t = 0.1$ s, and $\Delta t = 0.5$ s, the profit lost is \$7.42/h and \$7.86/h, respectively, which compares well with the continuous time case of \$7.29/h. In the case of $\Delta t = 0.1$ s, the discrete-time linear feedback generated by problem (31) is

$$L^* = Y^* (X^*)^{-1} = \begin{bmatrix} L_1^* & L_2^* \end{bmatrix}$$

$$L_1^* = \begin{bmatrix} -0.0382 & -0.491 & -783.6 & -988.4 & -0.124 & -156.7 \\ 0.420 & 0.0034 & 7.73 & -20.13 & -0.0893 & -43.70 \end{bmatrix} \times 10^{-3}$$

$$L_2^* = \begin{bmatrix} -16.92 & -54.32 & -0.166 & 148.05 & -0.0741 \\ -2.098 & -9.057 & 1.300 & 0.4201 & -0.00632 \end{bmatrix} \times 10^{-3} \tag{37}$$

The bottom plots of Figure 8 depict the result of a discrete-time simulation, using the linear model and the controller of (37). This scatter plot indicates very good agreement with the analytically determined EDOR (the solid line ellipse). Using the linearize version of the objective function and 15,000 data points, the numerically calculated profit loss is \$7.09/h, which seems to deviate from the \$7.42/h calculated analytically. However, if the simulation is increased to 80,000 data points, then the profit loss is calculated as \$7.46/h. The plot also illustrates a number of occasions in which the inequality constraints are violated. The next section will provide a method to remedy this problem.

Predictive Control with Full State Information

Conversion from statistically constrained control to the enforcement of point-wise-in-time constraints will require the use of Model Predictive Control (MPC). However,

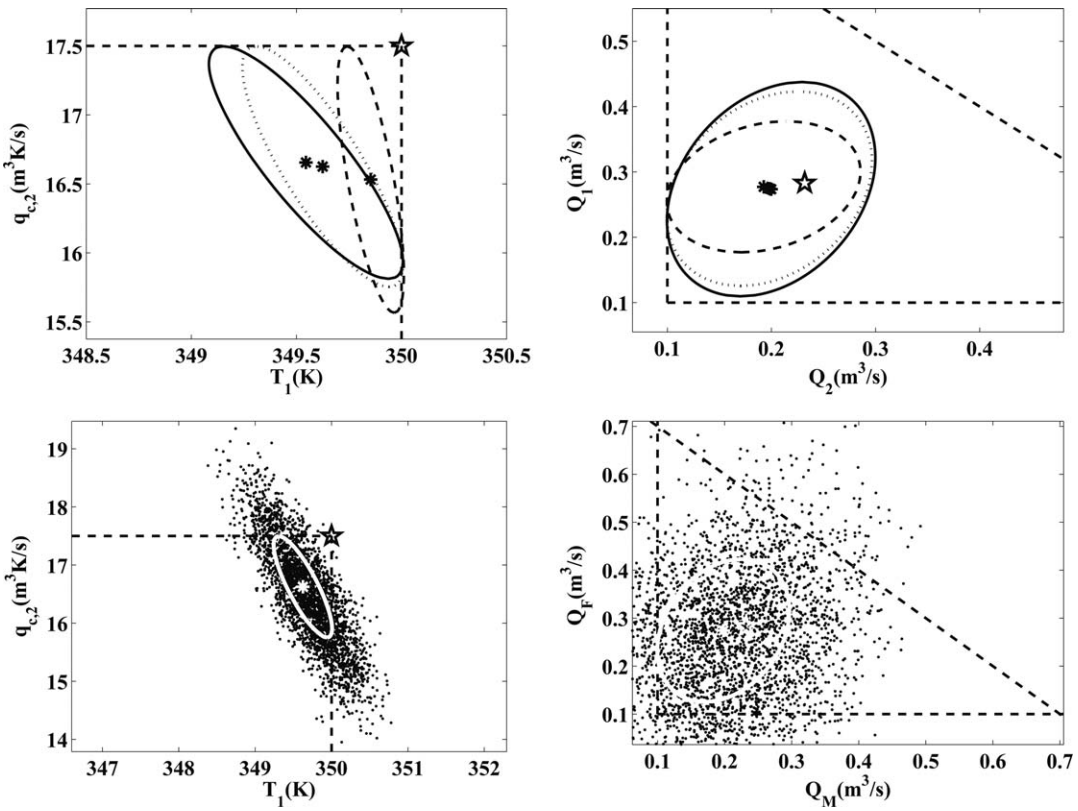

Figure 8. Illustration of discrete-time BOPs and EDORs for the free controller case.

Top plots: dotted, $\Delta t = 0.1$; dashed, $\Delta t = 0.5$; solid, continuous-time. Bottom plots, discrete-time simulation with $\Delta t = 0.1$.

special care must be used in constructing this controller, so as to arrive at an MPC generated EDOR that is similar to the one specified by the free controller BOP selection problem.

The notion of MPC is grounded in the concept of a predictive model

$$x_{k+1|i} = A_d x_{k|i} + B_d u_{k|i}, \quad k = i \ldots i+N-1, \tag{38}$$

$$z_{k|i} = D_x x_{k|i} + D_u u_{k|i}, \quad k = i \ldots i+N-1 \tag{39}$$

$$z^{\min} \le z_{k|i} \le z^{\max}, \quad k = i \ldots i+N-1 \tag{40}$$

$$x_{i|i} = x_i \tag{41}$$

where the time index k indicates predictive time and i is actual time ($z^{\min} = q^{\mathrm{BOP}} - q^{\min}$ and $z^{\max} = q^{\max} - q^{\mathrm{BOP}}$). The idea being that at time i, the state of the actual system, $x_{i+1} = A_d x_i + B_d u_i + G_d w_i$, is known to be x_i. Then, one would like to find a sequence of manipulations $u_{k|i}$, $k = i \ldots i+N-1$, such that the constraints (40) are satisfied. Once this sequence is determined, only the first manipulation, $u_{i|i}$, is sent to the process: $u_i = u_{i|i}$. Then, at time $i+1$, a new value for the initial condition, x_{i+1}, is obtained from the measurements and the process is repeated. However, as there are likely multiple sequences of $u_{k|i}$ satisfying the constraints, the sequence selection step is usually formulated as a quadratic program

$$\lim_{x_{k|i}, u_{k|i}} \sum_{k=i}^{i+N-1} \Phi(x_{k|i}, u_{k|i}) + x_{i+N|i}^T P x_{i+N|i} \quad \text{s.t.} \quad (38)(39)(40)(41) \tag{42}$$

where

$$\Phi(x_{k|i}, u_{k|i}) = \begin{bmatrix} x_{k|i} \\ u_{k|i} \end{bmatrix}^T \begin{bmatrix} Q & M \\ M^T & R \end{bmatrix} \begin{bmatrix} x_{k|i} \\ u_{k|i} \end{bmatrix} \tag{43}$$

and P is the positive definite solution to

$$P = A_d^T P A_d + Q - (M + A_d^T P B_d)(R + B_d^T P B_d)^{-1}(M + A_d^T P B_d)^T \tag{44}$$

Let us now consider the unconstrained version of problem (42), by removing constraints (40). In this case of unconstrained MPC, the feedback policy will be equal to the linear feedback generated by the LQR problem, $u_i = L_{\mathrm{LQR}} x_i$, where

$$L_{\mathrm{LQR}} = -(R + B_d^T P B_d)^{-1}(M + A_d^T P B_d)^T \tag{45}$$

Thus, to generate an unconstrained MPC policy with an EDOR identical to that specified by the free controller BOP selection problem, one need to only select MPC objective function weights, Q, R, and M, such that the LQR feedback, L_{LQR}, is equal to the feedback generated by problem (31), $L^* = Y^*(X^*)^{-1}$. In Ref. 51, it was shown that problem (31) will always generate a feedback, L^*, where such weights will exist. Then, synthesis of such weights can be achieved through the following theorem[57]

Theorem 3.1. *If there exists $P > 0$ and $R > 0$ such that*

$$\begin{bmatrix} P - A_d{}^T P A_d + L^T (R + B_d{}^T P B_d) L & L^T (R + B_d{}^T P B_d) + A_d{}^T P B_d \\ (L^T (R + B_d{}^T P B_d) + A_d{}^T P B_d)^T & R \end{bmatrix} > 0$$

Then $Q = P - A_d{}^T P A_d + L^T (R + B_d{}^T P B_d) L$ and $M = L^T (R + B_d{}^T P B_d) + A_d{}^T P B_d$ will be such that P and L satisfy (44) and (45) and

Table 3. Case Study Profit Losses

	Fixed Controller Profit Loss ($/h)	Free Controller Profit Loss ($/h)
Analytical	15.93	7.42
Unconstrained	17.08	7.09
Constrained	15.99	7.13

$$\begin{bmatrix} Q & M \\ M^T & R \end{bmatrix} > 0$$

Using the procedure of Theorem 3.1, objective function weights corresponding to the feedback of (37) were determined. Now that the linear feedback L^* has been exactly converted to the form of an unconstrained predictive controller it is a simple matter to reintroduce the point-wise-in-time constraints (40). The important point being that due to the selection of a BOP that is an appropriate distance from the constraints, the addition of point-wise-in-time constraints is expected to modify the EDOR only slightly.

Before demonstrating this similarity, the issue of infeasibility must be addressed. That is, there may exist initial conditions, $x_{i|i}$, such that the constraints $z^{\min} \le z_{k|i} \le z^{\max}$ cannot be satisfied for all $k = i,\ldots,i+N-1$. A popular approach to alleviate this issue is to implement a soft constrained version of MPC.[59] The method is to introduce a vector of slack variables $\theta_s \ge 0$ and replace (40) with

$$z^{\min} - \theta_s \le z_{k|i} \le z^{\max} + \theta_s \tag{46}$$

Then, the MPC objective function is augmented with $c_s^T \theta_s$, where c_s is a vector of positive constants. The impact of this soft constrained MPC formulation is that if c_s is sufficiently large, then θ_s will be very close to zero, except for cases in which the original MPC would be infeasible. In those cases, the constraints of (40) are relaxed, by (46), to determine a "reasonable" response to the infeasible initial condition. By appropriate selection of the terms within c_s, one can set priorities with regard to constraint relaxation. Roughly speaking, if the first element of c_s is 1–2 orders of magnitude smaller than the others, then the optimization will try to relax the first constraint before looking to the others.

Figure 9 demonstrates the performance of the soft constrained MPC algorithm. The top plots show the fixed controller using the tuning parameters, Q and R of Statistically Constrained Control Section, whereas the bottom plots show the free controller with tuning parameters determined from Theorem 3.1, both with a sample-time of 0.1 sec and $\tau_f = 10$ s. The impact of enforcing point-wise-in-time constraints is clearly observed in the manipulated variables, Q_1 and Q_2, as well as in T_1. In the $q_{c,2}$ direction, a number of constraint violations are observed. These violations are made possible by the soft constraint formulation and would result in an infeasible scenario if constraint softening was not available. A typical violation scenario begins with a low value at the disturbance $T_{c,2}$, which causes $q_{c,2}$ to increase. The controller responds by trying to reduce T_2, either directly by reducing Q_2 or indirectly by reducing Q_1, which will reduce T_1. This indirect route is clearly observed in the plots of Figure 9. However, as we did not soften the constraints on the manipulated variables, Q_1 and Q_2, the controller found it impossible to observe the $q_{c,2}$ constraint. Clearly, the constrained version of the free controller operates more within its analytically determined EDOR. This is due to the fact that the tuning parameters of the free controller were selected in the context of the constraints, and therefore,

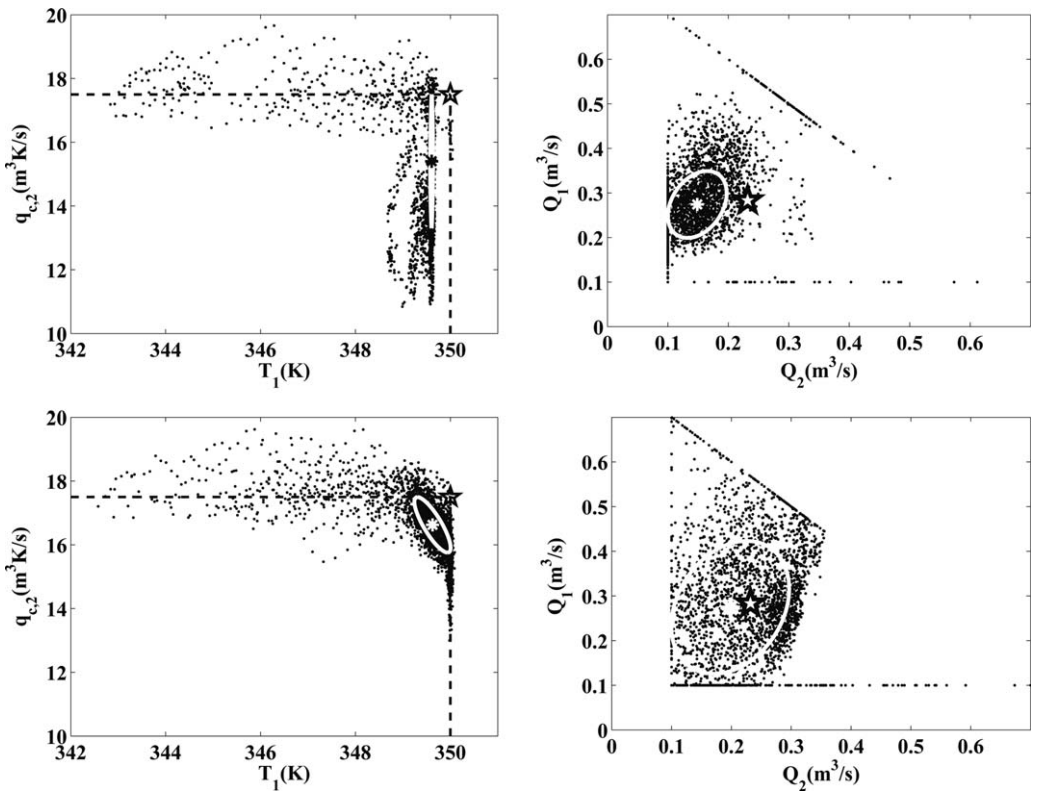

Figure 9. Constraint enforcement using MPC.

The top plots show the constrained fixed controller MPC, whereas the bottom shows the constrained free-controller MPC.

Table 4. Impact of EDOR Definition

α	Constrained	Unconstrained	% Violations of $q_{c,2}$
$\alpha = 0.5$	3.48	2.76	35.3%
$\alpha = 2$	22.28	22.39	2.5%
$\alpha = 1$ and α of $q_{c,2} = 2$	14.34	14.70	6.5%

when the constraints are active the controller is less erratic. This is also supported by the quantitative analysis: in the free controller case, the constrained profit loss is \$7.13/h and the unconstrained is \$7.09/h (both using 15,000 data points). In the fixed controller case, the loss is \$15.99/h and \$17.08/h for the constrained and unconstrained, respectively (Table 3).

Impact of EDOR definition

On first glance, it may appear that greater profit will result from a redefinition of the analytically calculated EDOR, dictated by the value of α in Eq. 33. For example, if α is set to 1/2, rather than 1, then the BOP will be selected closer to the OSSOP and the profit loss will be smaller (\$2.76/h for the unconstrained case and \$3.48/h for the constrained, see Table 4). However, the top plots of Figure 10 illustrate that such an approach will also result in an increase in constraint violations. Specifically, in the $q_{c,2}$ direction constraint violations increase from 20.1% to 35.3%. Similarly, one could select $\alpha = 2$, which would result in fewer constraint violations, but greater profit loss. The middle plots of Figure 10 illustrate constrained performance with $\alpha = 2$. This case results in $q_{c,2}$ violations of only 2.5%, but a profit loss of \$22.39/h (unconstrained) and \$22.28/h (constrained). It is interesting to note that setting $\alpha = 2$ for the fixed controller case resulted in an infeasible BOP selection problem. In fact, we could not find a set of diagonal Q and R matrices such that a feasible BOP could be found with $\alpha = 2$. A hybrid approach is to increase the α parameter only on the $q_{c,2}$ constraint. The result of this approach is shown in the bottom plots of Figure 10. In this case, the $q_{c,2}$ constraint violations are at 6.5% and the profit loss is \$14.70/h (unconstrained)

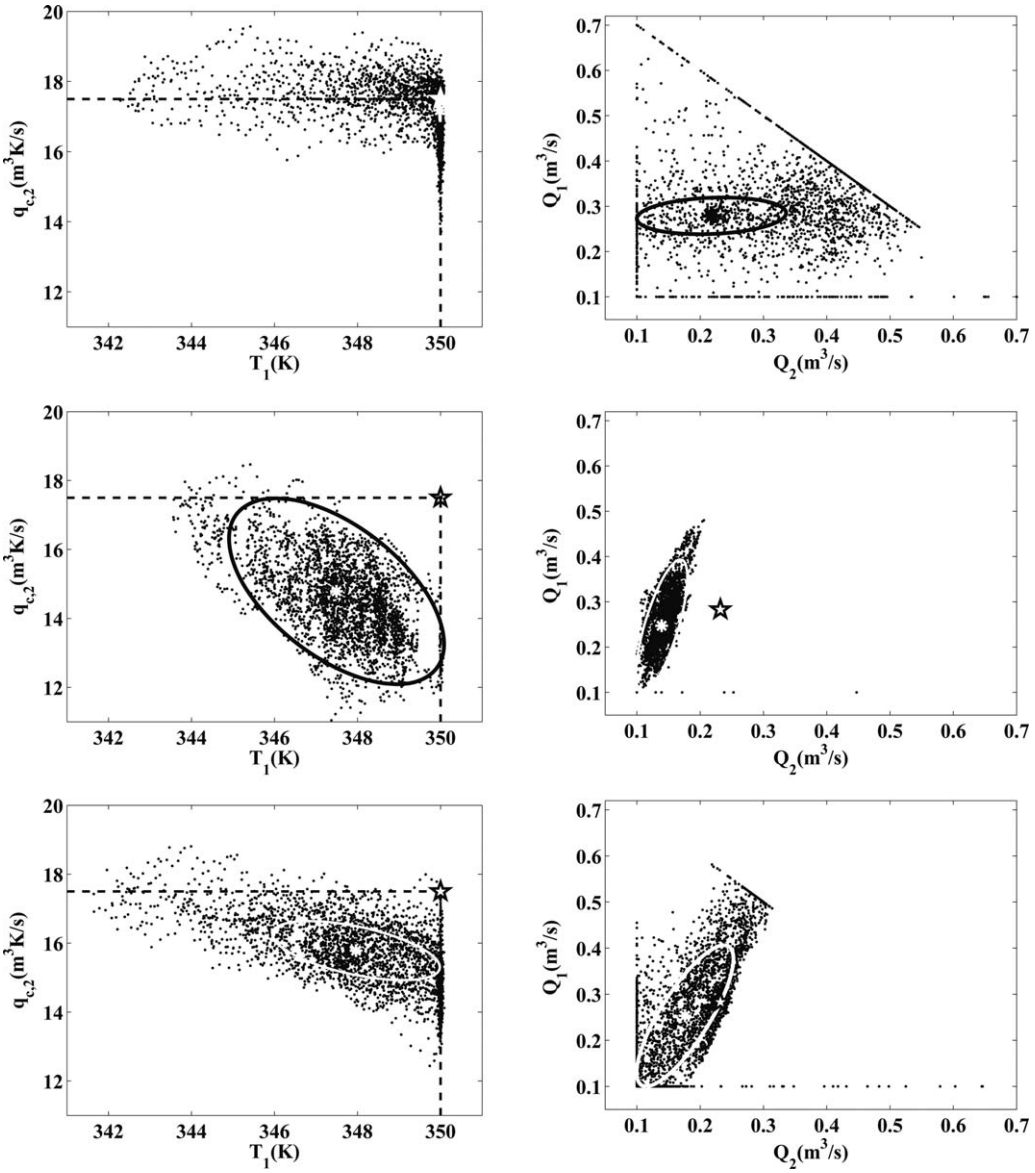

Figure 10. MPC simulations of various EDOR definitions, $\alpha = 0.5$ (top), $\alpha = 2$ (middle), and $\alpha = 2$ on the $q_{c,2}$ constraint (bottom).

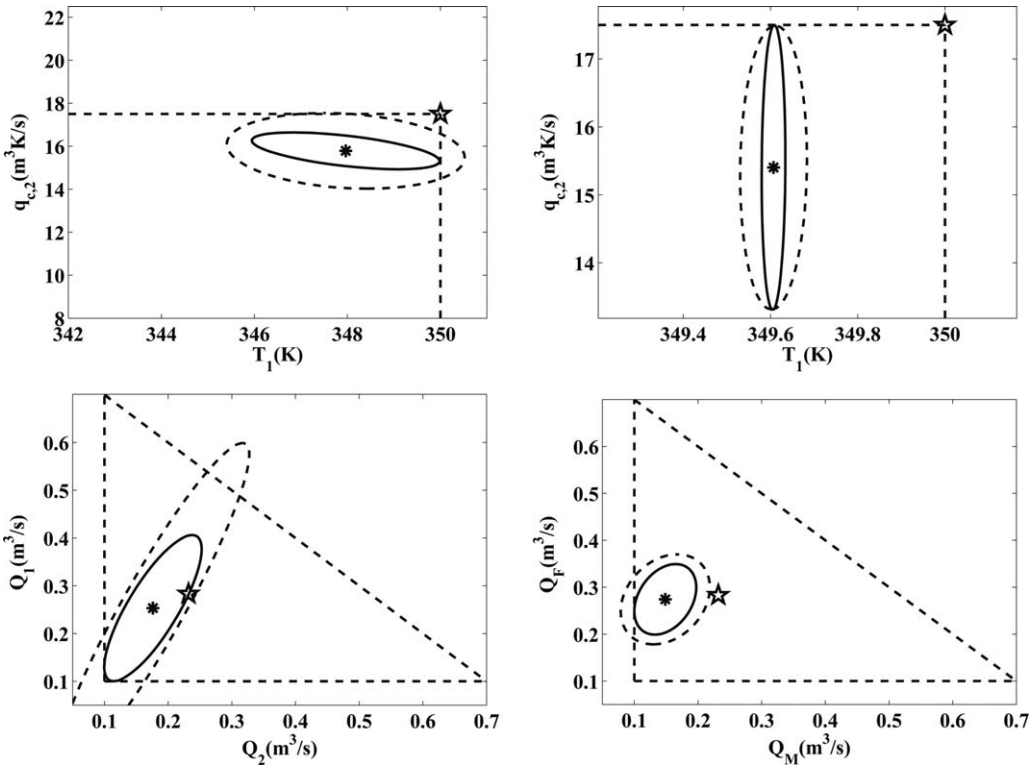

Figure 11. Impact of disturbance model mismatch Controllers designed with $\tau_f = 10$ and EDORs calculated using $\tau_f = 10$ (solid), $\tau_f = 1$ (dashed).

Left plots, free controller case; Right plots, fixed controller case.

and \$14.34/h (constrained). In all subsequent case study results, we will use this approach of $\alpha = 2$ in the $q_{c,2}$ direction and $\alpha = 1$ otherwise.

Disturbance model mismatch

In many cases, the correlation structure of the disturbances acting on the process will be unknown or may change over time. In the simple disturbance models discussed in the Statistically Constrained Control Section, this structure is defined by the time constant τ_f. To investigate sensitivity with respect to this parameter, simulations using a τ_f value different than the τ_f used to design the controller were performed. The plots of Figure 11 illustrate how the analytically determined EDORs will change if τ_f is changed from 10 to 1 s and the controller remains unchanged (designed using $\tau_f = 10$ s). In the free controller case, the EDOR in the $q_{c,2}$ direction increases, but not as much as one would expect based on the results of Figure 7. This is due to the controller's greater use of the manipulated variables, which now extend far beyond the inequality constraints of those variables. In the fixed controller case, the impact is much less dramatic. This can be attributed to the fact that the fixed controller makes almost no effort to regulate $q_{c,2}$ and thus has already paid the penalty in its section of a BOP. Note $\alpha = 1$ for all directions of the fixed controller case. In the scatter plots of Figure 12, we again see that the performance of the fixed controller is almost unchanged from Figure 9, although the constraint violations in the $q_{c,2}$ direction seem to be larger in magnitude, possibly due to the different placements for the BOPs in the two cases, recall Figure 6. In the free controller case, the magnitude of $q_{c,2}$ constraint violations appear to be similar to the fixed controller case. A quantitative assessment of the scatter plots indicates that the free controller has a profit loss of \$12.18/h and $q_{c,2}$ constraint violations at 24.6%, whereas the fixed controller has a loss of \$16.15/h and violations at 15.8%.

Clearly, the observations of this subsection, while informative, are purely anecdotal and the fact that the fixed controller appears to be more robust is less a result of intention and more a result of it being detuned with respect to the most important output of the process—$q_{c,2}$. If there is any conclusion, one can make it as the need for a robust formulation of the BOP selection problem, which would also consider process model mismatch. Using such an approach, the free controller case may be able to find a meaningful compromise between the $\tau_f = 1$ and $\tau_f = 10$ cases.

Modifications to the Measurement Structure

In this section, we remove the assumption of having perfect knowledge of the system state and illustrate how the BOP selection procedures should be modified to account for the expected measurement structure.

Computational delay

An important detail concerning MPC is the time required to numerically solve the quadratic program. In most cases, the sample time of the controller is selected so that the quadratic program can be solved within one sample period. The practical impact of requiring a sample period to determine the control action, u_i, is that x_i will not be known at the beginning of the computations. Specifically, the computations for u_i will begin at time $i-1$. Thus, the best one can do is predict x_i as

$$\bar{x}_i = A_d x_{i-1} + B_d u_{i-1} \tag{47}$$

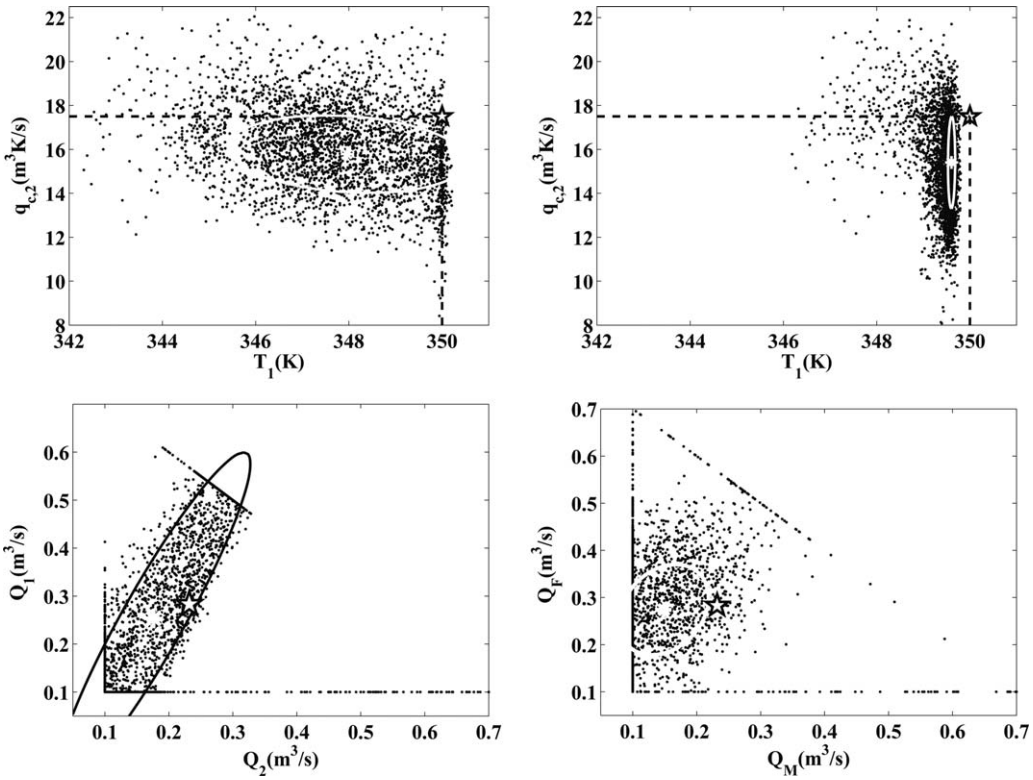

Figure 12. Impact of disturbance model mismatch.

Controllers designed with $\tau_f = 10$ and simulations with $\tau_f = 1$. Left plots, free controller; Right plots, fixed controller.

In the unconstrained case, the appropriate policy would be $u_i = L\bar{x}_i$. Using Eq. 30, one finds that $x_i = \bar{x}_i + G_d w_{i-1}$. Thus, Eq. 47 can be written as

$$\begin{aligned}\bar{x}_{i+1} &= A_d x_i + B_d u_i \\ &= A_d \bar{x}_i + A_d G_d w_{i-1} + B_d L \bar{x}_i \\ &= (A_d + B_d L)\bar{x}_i + A_d G_d w_{i-1}\end{aligned}$$

Similarly, the performance output can be written as $z_i = (D_x + D_u L)\bar{x}_i + D_x G w_{i-1}$. Thus, the free controller BOP selection problem, assuming a 1-step computational delay in Full State Information (FSI) measurements, is problem (31) with (35) and (36) replaced with

$$\begin{bmatrix} X - A_d G_d \Sigma_w G_d^T A_d & (A_d X + B_d Y) \\ (A_d X + B_d Y)^T & X \end{bmatrix} > 0 \tag{48}$$

$$\begin{bmatrix} \zeta_j - D_x G_d \Sigma_w G_d^T D_x^T & \rho_j (D_x X + D_u Y) \\ (D_x X + D_u Y)^T \rho_j^T & X \end{bmatrix} > 0 \quad j = 1 \ldots n_q \tag{49}$$

Using the delay-based linear feedback, a new set of objective function weights, Q, R, and M, can be generated, without modification of Theorem 3.1, and applied to the previous MPC algorithm with $x_{i|i} = \bar{x}_i$. The top plots of Figure 13 illustrate the impact of the delay. As on would expect the loss of profit is increased from \$15.10/h (undelayed) to \$15.67/h.

Predictive control with partial state information

In the partial state information (PSI) case, the control action will no longer be a function of the state, but rather a function of a noise corrupted measurement

$$y_i = C x_i + v_i \tag{50}$$

where v_i is a zero-mean white noise sequence with covariance Σ_v. In the unconstrained case, the appropriate policy is a linear feedback of the optimal state estimate: $u_i = L\hat{x}_i$, where $\hat{x}_i$ is generated from the steady-state Kalman filter[60,61]

$$\hat{x}_i = A_d \hat{x}_{i-1} + B_d u_{i-1} + K(y_i - C(A_d \hat{x}_{i-1} + B_d u_{i-1})) \tag{51}$$

The Kalman gain, K, is defined as

$$K = HC^T (CHC^T + \Sigma_v)^{-1} \tag{52}$$

$$H = A_d \Sigma_e A_d^T + G_d \Sigma_w G_d^T \tag{53}$$

$$\Sigma_e = H - HC^T (CHC^T + \Sigma_v)^{-1} CH \tag{54}$$

An important feature of the Kalman filter is that the innovations sequence, $\eta_i = y_i - C(A_d + B_d L)\hat{x}_{i-1}$, is a zero-mean white noise sequence with covariance $\Sigma_\eta = CHC^T + \Sigma_v$. Thus, the linear feedback, L, can be selected using the estimator based model

$$\hat{x}_{i+1} = (A_d + B_d L)\hat{x}_i + K\eta_{i+1} \tag{55}$$

$$z_i = (D_x + D_u L)\hat{x}_i + D_x(x_i - \hat{x}_i) \tag{56}$$

Then, using the fact that $\Sigma_e = E[(x_i - \hat{x}_i)(x_i - \hat{x}_i)^T]$ and $E[(x_i - \hat{x}_i)\hat{x}_i^T] = 0$, the free controller BOP selection problem, assuming PSI, is problem (31) with (35) and (36) replaced by

$$\begin{bmatrix} X + \Sigma_e - H & (A_d X + B_d Y) \\ (A_d X + B_d Y)^T & X \end{bmatrix} > 0 \tag{57}$$

$$\begin{bmatrix} \zeta_j - D_x \Sigma_e D_x^T & \rho_j (D_x X + D_u Y) \\ (D_x X + D_u Y)^T \rho_j^T & X \end{bmatrix} > 0 \quad j = 1 \ldots n_q \tag{58}$$

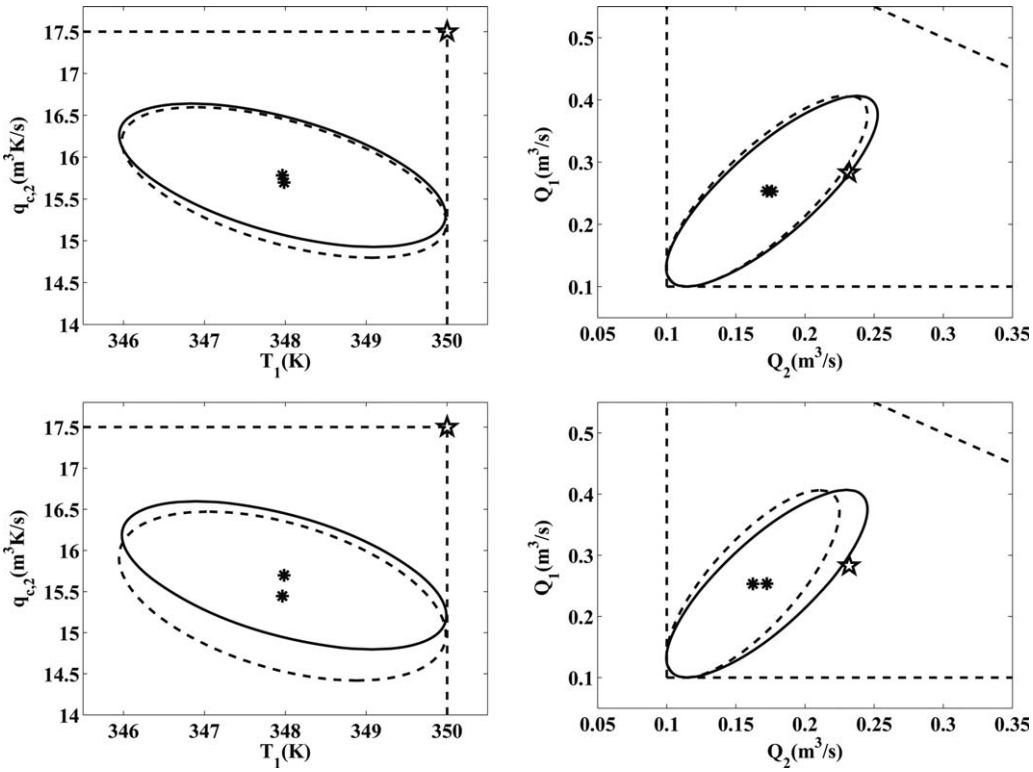

Figure 13. Impact of computational delay and PSI.

Top plots: full state information; Solid, undelayed; dashed, delayed. Bottom plots: delayed; solid, full state information; dashed, partial state information.

It is interesting to note that if $C = I$ and the limit is taken as $\Sigma_v \to 0$, then $\Sigma_e \to 0$, $H \to G_d \Sigma_w G_d^T$, and the above matrix inequalities will become identical to (35) and (36). To implement within MPC, one should recalculate the tuning parameters Q, R, and M in (43) based on the feedback gain $L = Y^*(X^*)^{-1}$ generated by the PSI free controller problem, and then set $x_{i|i} = \hat{x}_i$ in problem (42).

The above formulation of the PSI case assumes u_i is a function of $\hat{x}_i$ and ultimately of y_i, which carries the implicit assumption of zero computational delay. To arrive at the 1-step delay case, the feedback policy will be: $u_i = L\bar{\hat{x}}_i$, where $\bar{\hat{x}}_i$ is from the Kalman filter in its 1-step predictor form

$$\bar{\hat{x}}_i = A_d \bar{\hat{x}}_{i-1} + B_d u_{i-1} + A_d K(y_{i-1} - C\bar{\hat{x}}_{i-1}) \tag{59}$$

In this case, the exact same innovations sequence can be constructed as $\eta_i = y_i - C\bar{\hat{x}}_i$, but the covariance of the error signal is changed to $H = E[(x_i - \bar{\hat{x}}_i)(x_i - \bar{\hat{x}}_i)^T]$ and the orthogonality principle becomes $E[(x_i - \bar{\hat{x}}_i)\bar{\hat{x}}_i] = 0$. Thus, selection of the linear feedback, L, can utilize the following estimator based model

$$\bar{\hat{x}}_{i+1} = (A_d + B_d L)\bar{\hat{x}}_i + A_d K \eta_i \tag{60}$$

$$z_i = (D_x + D_u L)\bar{\hat{x}}_i + D_x\left(x_i - \bar{\hat{x}}_i\right) \tag{61}$$

The corresponding covariance equations are then found to be

$$\Sigma_{\bar{\hat{x}}} = (A_d + B_d L)\Sigma_{\bar{\hat{x}}}(A_d + B_d L)^T + A_d H C^T (CHC^T + \Sigma_v)^{-1} C H A_d^T \tag{62}$$

$$\Sigma_z = (D_x + D_u L)\Sigma_{\bar{\hat{x}}}(D_x + D_u L)^T + D_x H D_x^T \tag{63}$$

The net result is that the free controller BOP selection problem assuming PSI and a 1-step computational delay is problem (31) with (35) and (36) replaced by

$$\begin{bmatrix} X + A_d(\Sigma_e - H)A_d^T & (A_d X + B_d Y) \\ (A_d X + B_d Y)^T & X \end{bmatrix} > 0 \tag{64}$$

$$\begin{bmatrix} \zeta_j - D_x H D_x^T & \rho_j (D_x X + D_u Y) \\ (D_x X + D_u Y)^T \rho_j^T & X \end{bmatrix} > 0 \quad j = 1 \ldots n_q \tag{65}$$

It is additionally noted that setting $C = I$ and taking the limit as $\Sigma_v \to 0$ will cause the above inequalities to become identical to (48) and (49).

Returning to the case study, assume the measurement vector is $y = [T_1\ T_2\ T_f\ T_{c,1}\ T_{c,2}]^T$ and $\Sigma_v = \mathrm{diag}\{0.5^2\ 0.5^2\ 0.5^2\ 1\ 1\}$. Then, the bottom plots of Figure 13 compare the PSI case with the FSI, both with 1-step delay. As one would expect, the analytically determined profit loss is greater for the PSI case (from \$15.67/h to \$17.46/h). To implement within MPC, the resulting linear feedback should be converted to the corresponding objective function weights and $x_{i|i}$ should be set equal to $\bar{\hat{x}}_i$. Scatter plots of the soft constrained MPC policy with delayed PSI are given in the top plots of Figure 14. Clearly, the PSI controller has much greater difficulty observing the point-wise-in-time constraints and exhibits a behavior similar to the unconstrained case (bottom left plot of Figure 14). However, it should be highlighted that these plots indicate the actual values of system outputs, which in practice would be unmeasurable. The bottom right plot depicts the calculated state predictions (based on the state estimates) and more clearly illustrates the influence of the point-wise-in-time constraints.

Impact of Nonlinearities

This section begins with a comparison of the performance of the linear MPC on simulations based on the linear and

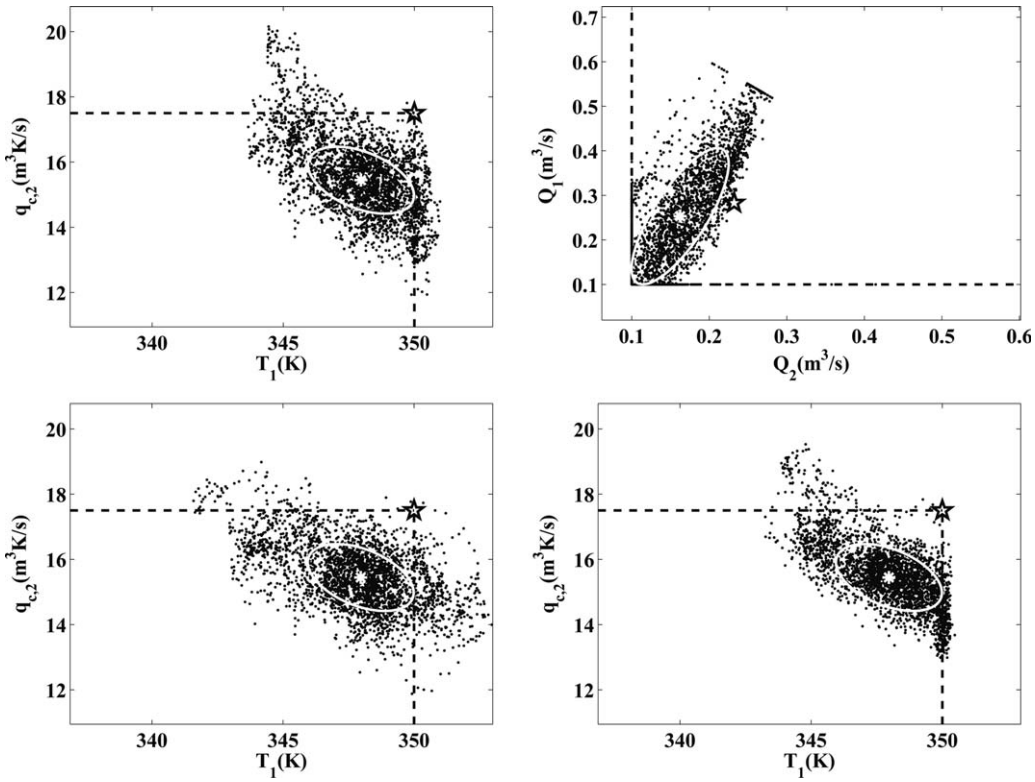

Figure 14. PSI controller.

Top plots: with point-wise-in time constraints. Bottom left: without point-wise constraint enforcement. Bottom right: output predictions with constraint enforcement.

nonlinear models. We then discuss a number of approaches that can be used to improve performance in the face of nonlinearities.

To simulate the nonlinear system of the Introduction Section, the MATLAB ODE solver is used. The general algorithm is as follows: before the simulation begins a BOP is selected and MPC tuning parameters are selected using the linearized model evaluated at the OSSOP. Then, at time $i-1$ an estimate of the state at the next time step, $\bar{\hat{x}}_i$, is determined using the measurement y_{i-1} and the linear state estimator. This estimate is used as the initial condition for the linear model-based MPC algorithm that selects the control action for the next time step, u_i. In addition, disturbance values are generated utilizing a linear stochastic discrete-time model driven by white noise. Using u_i and the generated disturbances, the nonlinear model is simulated for one time step. The state of the nonlinear simulation at the end of the time step is then used to generate the measurement y_i and the process is repeated. The plots of Figure 15 indicate that the discrepancy between the linear and nonlinear simulations is quite small. In fact, a scatter plot of the nonlinear simulation is almost impossible to distinguish from that of the linear simulation. Using the linearized version of g(q) the numerically calculated profit lost for the nonlinear simulation is \$14.50/h which compares well with the \$16.96/h calculated using the linear simulation. Use of the nonlinear version of g(q) to calculate profit results in a profit loss of \$17.20/h.

Incorporation of nonlinear characteristics

If the nonlinear model simulation resulted in significant discrepancy with respect to the linear model simulation, then one could apply any one of a number of alternate formulations. The first and likely most effective approach is to convert the MPC algorithm to a nonlinear MPC algorithm, by replacing Eqs. 38 and 39 with the nonlinear model. In this case, we continue to advocate that one should use the tuning parameters, Q, R, and M, as determined by the linear-based tuning method of the previous sections. The second alternative is to convert the linear-based state estimator to any one of a number of nonlinear state estimators. Again, no change to the MPC tuning parameters would be required, although a new value for the estimation error variance, Σ_e and H, may warrant a retuning based on (64) and (65). A third source of error can be attributed to the fact that the model was linearized around the OSSOP and not the BOP (as discussed in the Introduction Section). An appropriate approach to this issue is to make the linearized system matrices (g_q, A, B, D_x, D_u) a function of the BOP in problem (31). Unfortunately, this would add significantly to the complexity of problem (31). However, an *ad hoc* approach to such a problem, that has no guarantee of global optimality, is to relinearize the process model around the BOP determined from problem (31). Then, using this relinearization a new BOP could again be determined from (31). Figure 16 indicates that for the two-CSTR example this sort of iteration will essentially converge after the second relinearization.

Conclusions

This work demonstrates that the free controller tuning method can adapt well to each problem formulation explored. Even though the fixed controller tuning method gave similar results for the initial scenario of the case study, it was shown to adapt poorly to other scenarios. It was also shown that the free controller method was able to discover a

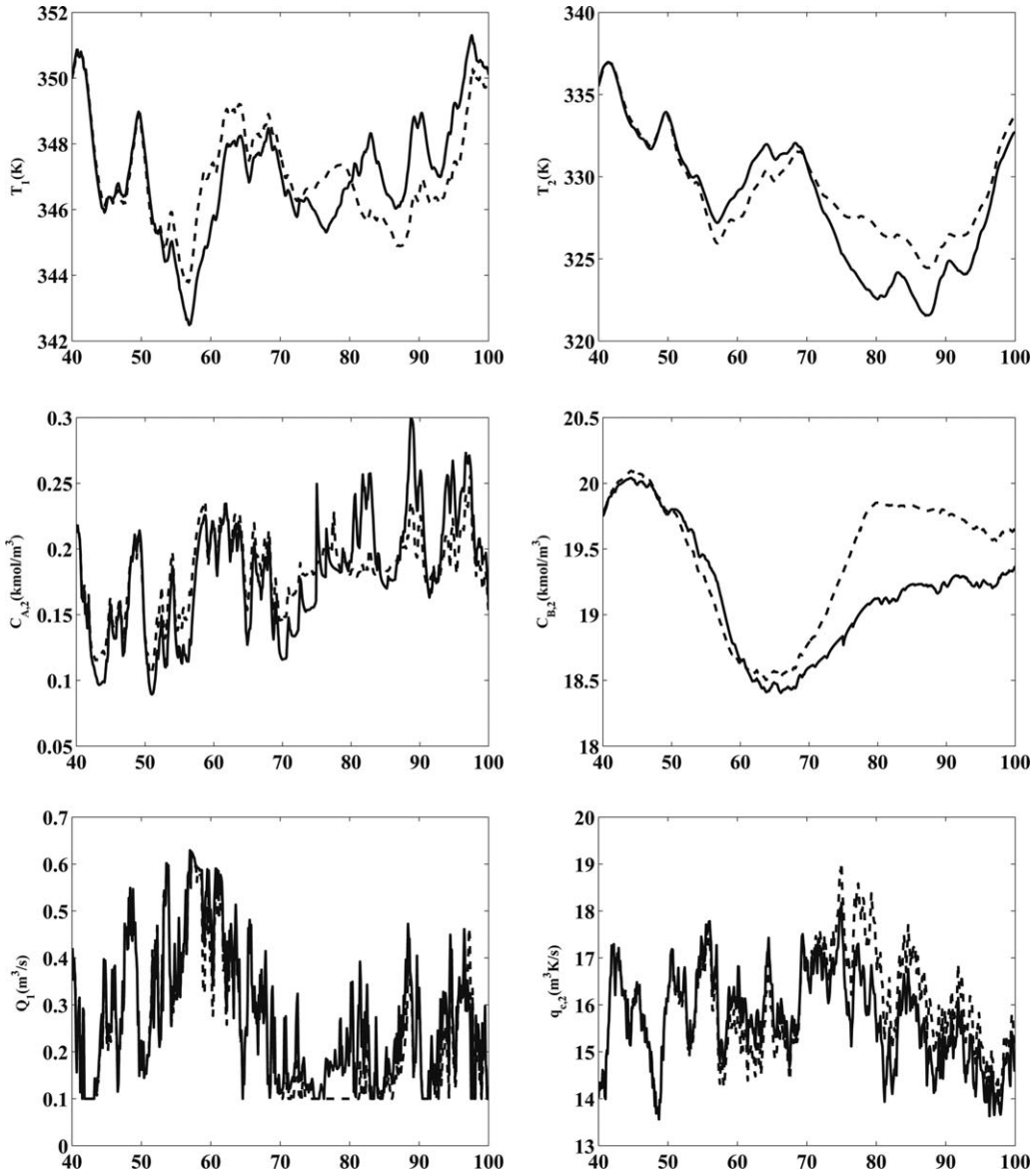

Figure 15. Comparison of linear a nonlinear model-based simulations.

Solid curve is nonlinear and dashed is linear.

multi-input approach to regulate one of the key outputs of the case study process, $q_{c,2}$. Specifically, it found that proper use of both manipulated variables could reduce the variability for this output and ultimately increase profit significantly. Although this discovery seems intuitive in hindsight, a fairly large amount of process understanding would be required for

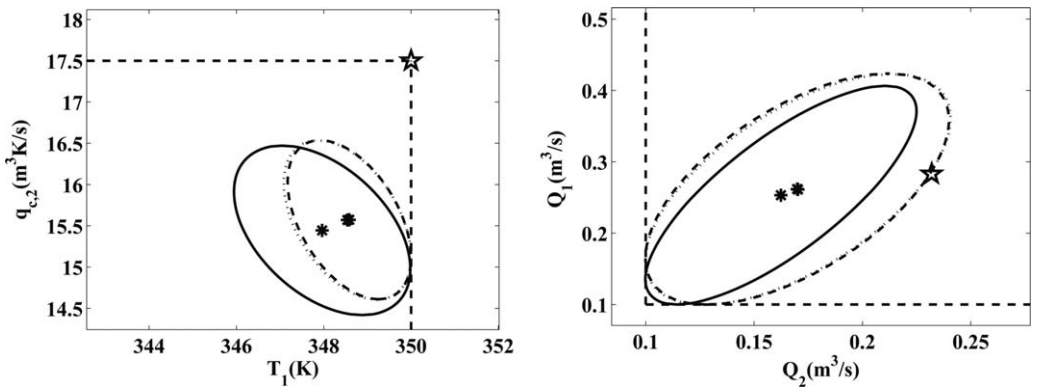

Figure 16. Evolution of BOP with relinearization.

(Solid, linearized around the OSSOP; Dashed, second iteration; dotted, third iteration).

one to propose such a tuning and significant analysis would be needed to identify when this approach should be used. Recall that this controller was only appropriate for $\tau_f \geq 10$ s. In contrast, the free controller approach was able to arrive at these conclusions with almost no effort.

It was also observed that the way the EDOR is defined (specifically the parameter α) will greatly influence the performance of the resulting controller. Although one may argue that we have merely shifted the tuning question from the objective function weights to these parameters (assuming each output may have a different α), the number of tuning parameters is significantly reduced and the new parameters provide a clear and easily understood trade-off between profit and constraint violation rates. Within this context, the area in need of improvement is in the quantitative measure of constraint violations. Specifically, a measure that considers magnitude of the violation along with probability would be beneficial.

The subsection on disturbance model mismatch clearly illustrates a need for future work on a robust formulation of the proposed free controller tuning method. Similarly, while the section on nonlinear impacts proposes an *ad hoc* "relinearize and iterate" approach, future work is warranted to develop a method to globally optimize the suggested tuning problem that accounts for nonlinearities in the steady-state model.

Acknowledgment

Both authors thank the National Science Foundation (CBET-0967906) for financial support.

Literature Cited

1. Nishida NA, Ichikawa A, Tazaki E. Synthesis of optimal process systems under uncertainty. *Ind Eng Chem Process Des Dev*. 1974; 13:209–214.
2. Grossmann I, Sargent RWH. Optimum design of chemical plants with uncertain parameters. *AIChE J*. 1978;24:1021–1028.
3. Polak E, Sangiovanni-Vincentelli A. Theoretical and computational aspects of the optimal design centering, tolerancing and tuning problem. *IEEE Trans Circuits Syst*. 1979;26:795–813.
4. Halemaane KP, Grossmann IE. Optimal process design under uncertainty. *AIChE J*. 1983;29:425–433.
5. Lasserre J, Roubellat F. Measuring decision flexibility in production planning. *IEEE Trans Autom Control*. 1985;AC-30:447–452.
6. Grossmann I, Floudas C. Active constraint strategy for flexibility analysis in chemical processes. *Comput Chem Eng*. 1987;11(6):675–693.
7. Raspantia C, Bandoni J, Biegler L. New strategies for flexibility analysis and design under uncertainty. *Comput Chem Eng*. 2000; 24(9–10):2193–2209.
8. Ostrovsky G, Achenie L, Wang Y, Volin Y. A new algorithm for computing process flexibility. *Ind Eng Chem Res*. 2000;39(7):2368–2377.
9. Malcolm A, Polan J, Zhang L, Ogunnaike B, Linninger A. Integrating systems design and control using dynamic flexibility analysis. *AIChE J*. 2007;53(8):2048–2061.
10. Pistikopoulos E, Grossmann I. Stochastic optimization of flexibility in retrofit design of linear system. *Comput Chem Eng*. 1988;12: 1215–1227.
11. Mohideen M, Perkins J, Pistikopoulos E. Optimal design of dynamic systems under uncertainty. *AIChE J*. 1996;42(8):2251–2272.
12. Ahmed S, Sahinidis N. Robust process planning under uncertainty. *Ind Eng Chem Res*. 1998;37:1883–1892.
13. Rooney W, Biegler L. Incorporating joint confidence regions into design under uncertainty. *Comput Chem Eng*. 1999;23(10):1563–1575.
14. Bansal V, Perkins J, Pistikopoulos E. Flexibility analysis and design using a parametric programming framework. *AIChE J*. 2002;48: 2851–2868.
15. Charnes A, Cooper W. Chance-constrained programming. *Manag Sci*. 1959;6:73–79.
16. Miller L, Wagner H. Chance-constrained programming with joint constraints. *Oper Res*. 1965;13:930–945.
17. Uryasev S. *Probabilistic Constrained Optimization: Methodology and Applications*. Dordrecht: Kluwer Academic Publishers, 2000.
18. Cooper W, Deng H, Huang Z, Li S. Chance constrained programming approaches to technical efficiencies and inefficiencies in stochastic data envelopment analysis. *J Oper Res Soc*. 2002;53:1347–1356.
19. Li P, Wendt M, Wozny G. Optimal planning for chemical engineering processes under uncertain market conditions. *Chem Eng Technol*. 2004;27:641–651.
20. Nemirovski A, Shapiro A. Convex approximations of chance constrained programming. *SIAM J*. 2006;17:969–996.
21. Li P, Arellano-Garciab H, Wozny G. Chance constrained programming approach to process optimization under uncertainty. *Comput Chem Eng*. 2008;32(1–2):25–45.
22. Morari M, Stephanopoulos G, Arkun Y. Studies in the synthesis of control structures for chemical processes, part I: promulgation of the problem. Process decomposition and the classification of the control task. Analysis of the optimizing control structures. *AIChE J*. 1980; 26(2):220–232.
23. Fisher W, Doherty M, Douglas J. The interface between design and control. 3. Selecting a set of controlled variables. *Ind Eng Chem Res*. 1988;27:611–615.
24. Stephanopoulos G, Ng C. Perspectives on the synthesis of plant-wide control structures. *J Process Control*. 2000;10:97–111.
25. Skogestad S. Self-optimizing control: the missing link between steady-state optimization and control. *Comput Chem Eng*. 2000; 24(2–7):569–575.
26. Chodavarapu S, Zheng A. A definition of steady-state plant-wide controllability. *Ind Eng Chem Res*. 2002;41:4338–4345.
27. Ward J, Mellichamp D, Doherty M. Insight from economically optimal steady-state operating policies for dynamic plantwide control. *Ind Eng Chem Res*. 2006;45:1343–1354.
28. Mellefont D, Sargent R. Selection of measurements for optimal feedback control. *Ind Eng Chem Process Des Dev*. 1978;17:549–552.
29. Harris T, Macgregor J, Wright J. Optimal sensor location with an application to a packed bed tubular reactor. *AIChE J*. 1980;26(6): 910–916.
30. Morari M, Stephanopoulos G. Studies in the synthesis of control structures for chemical processes, part III: optimal selection of secondary measurements within the framework of state estimation in the presence of persistent unknown disturbances. *AIChE J*. 1980;26: 247–260.
31. Romagnoli J, Alvarez J, Stephanopolus G. Variable measurement structures for process control. *Int J Control*. 1981;33:269–289.
32. Narraway L, Barton JPG. Interaction between process design and process control: economic analysis of process dynamics. *J Process Control*. 1991;1:243–250.
33. Hovd M, Skogestad S. Procedure for regulatory control structure selection with application to the FCC process. *AIChE J*. 1993; 39(12):1938–1953.
34. Narraway L, Perkins J. Selection of process control structure based on economics. *Comput Chem Eng*. 1994;18:511–515.
35. Lee J, Braatz R, Morari M, Packard A. Screening tools for robust control structure selection. *Automatica*. 1995;31(2):229–235.
36. Loeblein C, Perkins J. Economic analysis of different structures of on-line process optimization systems. *Comput Chem Eng*. 1998; 22(9):1257–1269.
37. Loeblein C, Perkins J. Structural design for on-line process optimization: I. Dynamic economics of MPC. *AIChE J*. 1999;45(5):1018–1029.
38. Heath J, Kookos I, Perkins J. Process control structure selection based on economics. *AIChE J*. 2000;46(10):1998–2016.
39. Seferlis P, Grievink J. Process design and control structure screening based on economic and static controllability criteria. *Comput Chem Eng*. 2001;25:177–188.
40. Kookos I, Perkins JD. An algorithmic method for the selection of multivariable process control structures. *J Process Control*. 2002; 12(1):85–99.
41. Peng J, Chmielewski D. Covariance based hardware selection-part II: equivalence results for the sensor, actuator and simultaneous selection problems. *IEEE Trans Control Syst Technol*. 2006;14(2):362–368.
42. Bahri P, Bandoni J, Barton G, Romagnoli J. Back-off calculations in optimizing control: a dynamic approach. *Comput Chem Eng*. 1995; 19:S699–S708.

43. Young J, Swartz C, Ross R. On the effects of constraints, economics and uncertain disturbances on dynamic operability assessment. *Comput Chem Eng*. 1996;20:S667–S682.
44. Bahri P, Bandoni J, Romagnoli J. Effect of disturbances in optimizing control: steady-state open-loop backoff problem. *AIChE J*. 1996; 42(4):983–994.
45. Figueroa J, Bahri P, Bandoni J, Romagnoli J. Economic impact of disturbances and uncertain parameters in chemical processes - a dynamic back-off analysis. *Comput Chem Eng*. 1996;20(4):453–461.
46. Figueroa J, Desages A. Dynamic 'back-off' analysis: use of piecewise linear approximations. *Optim Control Appl Methods*. 2003;24: 103–120.
47. Rooney W, Biegler L. Optimal process design with model parameter uncertainty and process variability. *AIChE J*. 2003;49(2):438–449.
48. Arbiza M, Bandoni J, Figueroa J. Use of back-off computation in multilevel MPC. *Lat Am Appl Res*. 2003;33:251–256.
49. van Hessem D, Scherer C, Bosgra O. LMI-based closed-loop economic optimization of stochastic process operation under state and input constraints. *Sel Topic Signals Syst Control*. 2001;12:31–38.
50. Muske K. Estimating the economic benefit from improved process control. *Ind Eng Chem Res*. 2003;42:4535–4544.
51. Peng JK, Manthanwar A, Chmielewski D. On the tuning of predictive controllers: the minimum back-off operating point selection problem. *Ind Eng Chem Res*. 2005;44:7814–7822.
52. Lee K, Huang B, Tamayo E. Sensitivity analysis for selective constraint and variability tuning in performance assessment of industrial MPC. *Control Eng Pract*. 2008;16(10):1195–1215.
53. Zhao C, Zhao Y, Su H, Huang B. Economic performance assessment of advanced process control with LQG benchmarking. *J Process Control*. 2009;19(4):557–569.
54. Akande S, Huang B, Lee K. MPC constraint analysis-bayesian approach via a continuous-valued profit function. *Ind Eng Chem Res*. 2009;48(8):3944–3954.
55. Nabil M, Narasimhan S, Skogestad S. Economic back-off selection based on optimal multivariable controller. *Proceedings of the 8th International IFAC Symposium on Advanced Control of Chemical Processes (ADCHEM)*. Furama Riverfront, Singapore, 2012.
56. Peng J, Chmielewski D. Optimal sensor network design using the minimally backed-off operating point notion of profit. *Proceedings of the American Control Conference*. Portland, OR, 2005.
57. Chmielewski D, Manthanwar A. On the tuning of predictive controllers: inverse optimality and the minimum variance covariance constrained control problem. *Ind Eng Chem Res*. 2004;43:7807–7814.
58. Burl J. *Linear Optimal Control*. Menlo Park, CA: Addison Wesley, 1999.
59. Zheng A, Morari M. Stability of model predictive control with mixed constraints. *IEEE Trans Autom Control*. 1995;40(10):1818–1823.
60. Anderson B, Moore J. *Optimal Filtering*. Englewood Cliffs, NJ: Prentice-Hall, 1979.
61. Balakrishnan A. *Kalman Filtering Theory*. New York, NY: Optimization Software, Inc., 1987.

Appendix

The submatrices of Eqs. 28 and 29. All variables are evaluated at $s = s^{\mathrm{OSSOP}}$, $m = m^{\mathrm{OSSOP}}$, and $p = p^{\mathrm{OSSOP}}$

$$A_{11}=\begin{bmatrix} -\frac{Q_1}{V}-\frac{\partial r_A}{\partial C_{A,1}} & 0 & -\frac{\partial r_A}{\partial T_1} \\ \frac{\partial r_A}{\partial C_{A,1}} & -\frac{Q_1}{V}-\frac{\partial r_B}{\partial C_{B,1}} & \frac{\partial r_A}{\partial T_1}-\frac{\partial r_B}{\partial T_1} \\ H_A\frac{\partial r_A}{\partial C_{A,1}} & H_B\frac{\partial r_B}{\partial C_{B,1}} & -\frac{Q_1}{V}-H_A\frac{\partial r_A}{\partial T_1}-H_B\frac{\partial r_B}{\partial T_1}-U_a \end{bmatrix}$$

$$A_{22}=\begin{bmatrix} -\frac{Q_T}{V}-\frac{\partial r_A}{\partial C_{A,2}} & 0 & -\frac{\partial r_A}{\partial T} \\ \frac{\partial r_A}{\partial C_{A,2}} & -\frac{Q_1}{V}-\frac{\partial r_B}{\partial C_{B,2}} & \frac{\partial r_A}{\partial T_2}-\frac{\partial r_B}{\partial T_2} \\ H_A\frac{\partial r_A}{\partial C_{A,2}} & H_B\frac{\partial r_B}{\partial C_{B,2}} & -\frac{Q_T}{V}-H_A\frac{\partial r_A}{\partial T_2}-H_B\frac{\partial r_B}{\partial T_2}-U_a \end{bmatrix}$$

$$A_{21}=\begin{bmatrix} \frac{Q_1}{V} & 0 & 0 \\ 0 & \frac{Q_1}{V} & 0 \\ 0 & 0 & \frac{Q_1}{V} \end{bmatrix}$$

$$B_1=\begin{bmatrix} \frac{C_{A,F}-C_{A,1}}{V} & 0 \\ -\frac{C_{B,1}}{V} & 0 \\ \frac{T_F-T_1}{V} & 0 \end{bmatrix}, B_2=\begin{bmatrix} \frac{C_{A,1}-C_{A,2}}{V} & \frac{C_{A,F}-C_{A,2}}{V} \\ \frac{C_{B,1}-C_{B,2}}{V} & -\frac{C_{B,2}}{V} \\ \frac{T_1-T_2}{V} & \frac{T_F-T_2}{V} \end{bmatrix}$$

$$G_1=\begin{bmatrix} 0 & \frac{Q_1}{V} & 0 & 0 & 0 \\ 0 & 0 & 0 & 0 & -r_B\left(T_1,C_{B,1}\right)/k_{B,II} \\ \frac{Q_1}{V} & 0 & U_a & 0 & -H_B r_B\left(T_1,C_{B,1}\right)/k_{B,II} \end{bmatrix}$$

$$G_2=\begin{bmatrix} 0 & \frac{Q_2}{V} & 0 & 0 & 0 \\ 0 & 0 & 0 & 0 & -r_B\left(T_2,C_{B,1}\right)/k_{B,II} \\ \frac{Q_2}{V} & 0 & 0 & U_a & -H_B r_B\left(T_2,C_{B,1}\right)/k_{B,II} \end{bmatrix}$$

and D_x, D_u, and D_w is given by

$$D_{x,1}=\begin{bmatrix} 0&0&1&0&0&0 \\ 0&0&0&1&0&0 \\ 0&0&0&0&1&0 \\ 0&0&0&0&0&1 \end{bmatrix},\ D_{u,2}=\begin{bmatrix} 1&1 \\ 1&0 \\ 0&1 \end{bmatrix}$$

$$D_{x,3}=\begin{bmatrix} 0&0&U_a&0&0&0 \\ 0&0&0&0&0&U_a \end{bmatrix}, D_{w,3}=\begin{bmatrix} 0&0&-U_a&0&0 \\ 0&0&0&-U_a&0 \end{bmatrix}$$

Manuscript received Oct. 4, 2013, and revision received Apr. 16, 2014.